

Accepted Manuscript

Novel 4-(4-substituted amidobenzyl)furan-2(5H)-one derivatives as topoisomerase I inhibitors

Cheng-Kang Peng, Ting Zeng, Xing-Jun Xu, Yi-Qun Chang, Wen Hou, Kuo Lu, Hui Lin, Ping-Hua Sun, Jing Lin, Wei-Min Chen



PII: S0223-5234(16)31042-X

DOI: [10.1016/j.ejmech.2016.12.035](https://doi.org/10.1016/j.ejmech.2016.12.035)

Reference: EJMECH 9126

To appear in: *European Journal of Medicinal Chemistry*

Received Date: 25 September 2016

Revised Date: 13 December 2016

Accepted Date: 17 December 2016

Please cite this article as: C.-K. Peng, T. Zeng, X.-J. Xu, Y.-Q. Chang, W. Hou, K. Lu, H. Lin, P.-H. Sun, J. Lin, W.-M. Chen, Novel 4-(4-substituted amidobenzyl)furan-2(5H)-one derivatives as topoisomerase I inhibitors, *European Journal of Medicinal Chemistry* (2017), doi: 10.1016/j.ejmech.2016.12.035.

This is a PDF file of an unedited manuscript that has been accepted for publication. As a service to our customers we are providing this early version of the manuscript. The manuscript will undergo copyediting, typesetting, and review of the resulting proof before it is published in its final form. Please note that during the production process errors may be discovered which could affect the content, and all legal disclaimers that apply to the journal pertain.

Graphical Abstract

Novel 4-(4-substituted amidobenzyl)furan-2(5H)-one derivatives as topoisomerase I inhibitors

Cheng-Kang Peng¹, Ting Zeng¹, Xing-Jun Xu, Yi-Qun Chang, Wen Hou, Kuo Lu, Hui Lin, Ping-Hua Sun, Jing Lin*, Wei-Min Chen*

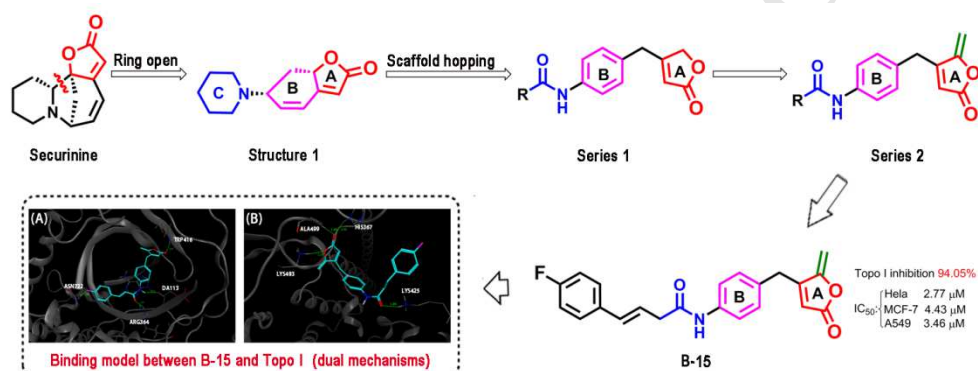
College of Pharmacy, Jinan University, Guangzhou 510632, P. R. China

¹ These authors contributed equally to this work.

*Corresponding authors. Tel.: +86 20 8522 1367(J. Lin), +86 20 8522 4497 (W.-M. Chen).

Fax: +86 20 8522 4766.

E-mail address: linjing_jnu@163.com (J. Lin), twmchen@jnu.edu.cn(W.-M. Chen).



Novel 4-(4-substituted amidobenzyl)furan-2(5H)-one derivatives as topoisomerase I inhibitors

Cheng-Kang Peng¹, Ting Zeng¹, Xing-Jun Xu, Yi-Qun Chang, Wen Hou, Kuo Lu, Hui Lin,

Ping-Hua Sun, Jing Lin*, Wei-Min Chen*

College of Pharmacy, Jinan University, Guangzhou 510632, P. R. China

¹ These authors contributed equally to this work.

*Corresponding authors. Tel.: +86 20 8522 1367(J. Lin), +86 20 8522 4497 (W.-M. Chen).

Fax: +86 20 8522 4766.

E-mail address: linjing_jnu@163.com (J. Lin), twmchen@jnu.edu.cn(W.-M. Chen).

ABSTRACT

In this study, two series of novel 4-(4-substituted amidobenzyl)furan-2(5H)-one derivatives containing an α,β -unsaturated lactone fragment were synthesized and screened for Topo I inhibition and antitumor activity. The topoisomerase I inhibitory activities and cytotoxicities against three human cancer cell lines (MCF-7, HeLa, A549) were evaluated. The results revealed that series **2**, compounds bearing an exocyclic double bond on the furanone ring, generally showed more potent activity than series **1**, compounds lacking an exocyclic double bond. Several compounds of series **2** possess significant Topo I inhibitory activity and potent antiproliferative activity against cancer cell lines. Further mechanism studies of the most active compound of series **2** (**B-15**) indicated that synthetic compounds can not only stabilize the drug-enzyme-DNA covalent ternary complex as well as camptothecin, but also interfere with the binding between Topo I and DNA. The binding patterns of these compounds with Topo I and structure-activity relationships are discussed.

Keywords: Furan-2(5H)-one; α , β -unsaturated lactones; Topoisomerase I; Antitumor

1. Introduction

Cancer is one of the leading global health problems worldwide with an increasing number of patients every year [1]. The current oncotherapy methods include radiotherapy, immunotherapy, surgery and chemotherapy, and the design and synthesis of new drugs for the treatment of cancer is a crucial area of research in medicinal chemistry [2].

Topoisomerase I (Topo I) is a ubiquitous nuclear enzyme that catalyzes transient cleavage and reconnection in DNA, events which are associated with DNA replication, transcription, recombination and chromatin remodeling [3,4]. Evidence suggests that DNA topoisomerase I is an effective target for the discovery of antitumor drugs as a result of its high over-expression in cancer cells [5-8].

Compounds bearing α,β -unsaturated lactones or 2-furanone (**Fig. 1**) have been reported to have a broad spectrum of biological roles, including antitumor, antibacterial, and anti-inflammatory activities [9], which suggests that the α,β -unsaturated lactone is a promising pharmacophore for drug design. Other studies have revealed that compounds bearing an α,β -unsaturated lactone fragment, such as some cardiac glycosides, acetogenins and securinines could serve as Topo I inhibitors [7,10,11]. Meanwhile, several reports have revealed that exocyclic double bonds are an essential structural feature which increases antitumor activity [12,13]. Many clinical trials have been conducted of anticancer drugs, such as Eribulin [14], calicheamicin [15], all of which contain an exocyclic double bond. In this study, two series of 4-(4-substituted amidobenzyl)furan-2(5H)-one derivatives bearing an α,β -unsaturated lactone fragment (**Fig. 1**, Series **1**: without exocyclic double bond; Series **2**: with exocyclic double bond) have been designed, synthesized and evaluated as Topo I inhibitors.

The topoisomerase I inhibitory activity and the cytotoxicity against three human cancer cell lines (MCF-7, HeLa, A549) of the synthesized compounds was evaluated and several compounds that show both excellent Topo I inhibitory activity and effective potent antiproliferative activity against cancer cell lines were identified. The novel dual action mechanism on Topo I of these 4-(4-substituted

amidobenzyl)furan-2(5H)-one derivatives was illuminated by three different electrophoresis experiments and docking studies. In addition, the structure-activity relationships of these compounds are discussed.

2. Chemistry

The design strategy for 4-(4-substituted amidobenzyl)furan-2(5H)-one derivatives is shown in **Fig. 1**. Securinine bearing an α,β -unsaturated lactone, extracted from *securinega* [16], shows potent antiproliferative activity as a Topo I inhibitor [7,17,18] suggesting that securinine may be used as a lead compound for the development of topoisomerase I inhibitors as antitumor agents. An attempt was made to simplify the structure of securinine and design target compounds whose structure can be easily synthesized. First, the bond between C2 and C9 of securinine was opened, producing structure **1**. A molecular docking study using *Sybyl-8.1* was performed to investigate the interaction between structure **1** and Topo I (PDB: 1K4T). Guided by the docking results (shown in Supporting Information, SI), compounds in series **1** were designed by scaffold hopping from structure **1**. Rings B and C of structure **1** were replaced with a phenyl ring and an amido bond. The amide is connected to the phenyl ring by a variable length linker. In series **1**, C4 of the furanone ring is a linear hydrocarbon, while in series **2**, C4 of the furanone ring was modified to produce an exocyclic double bond to assess whether such an exocyclic double bond is related to antitumor activity. The synthesis of the designed compounds in **Fig. 1** is outlined in **Scheme 1** (series **1**: **A-1~A-7**) and **Scheme 2** (series **2**: **B-1~B-15**).

[Figure 1]

2.1. Synthesis of the target compounds, series 1

3-Phenylpropanal was reacted with glyoxylic acid monohydrate and potassium hydroxide in dichloromethane at room temperature affording (*Z*)-3-benzyl-4-oxobut-2-enoic acid (**1-1**) [19]. Compound **1-1**, treated with nitrosnitric acid at -10 °C afforded the *p*-nitrophenyl compound **1-2**, which was reduced to the hydroxyl

compound (**1-3**) with sodium borohydride in methanol at 0 °C [20]. Compound **1-3** with *N*-(3-dimethylaminopropyl)-*N'*-ethylcarbodiimide hydrochloride (EDCI) in dry dichloromethane at room temperature afforded 4-(4-nitrobenzyl)furan-2(5H)-one (**1-4**), which was reduced to 4-(4-aminobenzyl)-furan-2(5H)-one (**1-5**) with iron and ammonium chloride in ethanol at 80 °C [21]. This compound (**1-5**), treated with acyl chloride and dry pyridine in tetrahydrofuran at 0 °C afforded the amides **A-1~A-7** [22].

[Scheme 1]

Synthesis of the target compounds series 2

Reaction of 1-(bromomethyl)-4-nitrobenzene with 2,4-pentanedione in methanol at 75 °C gave 4-(4-nitrophenyl)butan-2-one (**2-1**) which, treated with glyoxylic acid monohydrate in phosphoric acid at 85 °C afforded compound **2-2**. This was refluxed with *p*-toluenesulfonic acid in toluene to afford 5-methylene-4-(4-nitrobenzyl)furan-2(5H)-one (**2-3**) [23]. This was refluxed with iron and ammonium chloride in ethanol to obtain the amine **2-4** [21] which, with the appropriate acyl chloride and dry pyridine in tetrahydrofuran at 0 °C afforded the target compounds **B-1~B-15** [22].

[Scheme 2]

All the compounds were fully analyzed and characterized by ¹H NMR, ¹³C NMR, mass spectrometry (MS) and high resolution mass spectrometry (HRMS).

3. Results and Discussion

3.1. Topo I inhibitory activity

It has been reported that Topo I is one of the targets of compounds bearing a 2-furanone with an α,β -unsaturated lactone [9]. Consequently, a DNA relaxation assay was used to investigate the inhibition of Topo I by 4-(4-substituted amidobenzyl)furan-2(5H)-one derivatives. As shown in **Fig. 2A**, the Topo I inhibitory activity is directly related to the conversion of supercoiled DNA to its relaxed form

[24]. Camptothecin (CPT), a well-known Topo I inhibitor, was chosen as a positive control. As shown in **Fig. 2A**, when treated with 100 μ M of various furanone derivatives, inhibition of Topo I between 11-94%, revealed by gray scale value analysis, shown in **Table 1**, is observed. Notably, the most active compound is **B-15** which showed an inhibition rate of 94.04% at 100 μ M, significantly higher than that of the positive control CPT (79.50% at 100 μ M). In addition, compounds **B-3**, **B-5**, **B-8**, **B-12**, **B-13** exhibited considerable activity, with inhibition rates of 47.94%, 41.93%, 43.32%, 48.64%, and 44.62% respectively. However, compounds of series **1** that lack the exocyclic double bond generally showed poor inhibitory activity, with inhibition rates <20%. These results show that introduction of exocyclic double bond improves the Topo I inhibitory activity of 4-(4-substituted amido-benzyl)-furan-2(5H)-one derivatives. We then applied the most active compound (**B-15**) to a concentration gradient experiment, shown in **Fig. 3** and found that the inhibition rate of **B-15** decreased linearly in a concentration-dependent manner. Based on the results of Topo I inhibitory activity, the structure-activity relationship of the furanone derivatives can be summarized as follows: (1) introduction of exocyclic double bond dramatically improves the Topo I inhibitory activity; (2) the longer the carbon chain in the furanone derivatives, the higher the inhibitory activity; (3) substitution of both electron withdrawing groups or electron donating groups at the *para*-position of the phenyl ring can improve the Topo-I inhibitory activity.

[Table 1]

[Figure 2]

[Figure 3]

To determine if the exocyclic double bond is essential to the Topo I inhibitory activity, a molecular docking study was performed with *Sybyl-8.1* [25] to clarify the possible interaction mode between the furanone derivatives and Topo I (PDB: 1K4T). The complexes were validated by molecular dynamics (MD) simulation (RMSD plots were shown in **Figure S2**) and the free binding energy (ΔG) was calculated afterward (**Table S1**). As shown in **Fig. 4**, the furanone rings of the active

compounds (**B-13**, **B-14**, **B-15**) were selected as representatives of the compounds in series **2**. These compounds could interact with the active pocket of Topo I by π - π stacking or the π -alkyl stacking. However, no π - π stacking interactions or π -alkyl stacking interactions could be observed between compounds in series **1** and the active pocket of Topo I (data not shown), which probably because removing the double-bond broken the cyclic conjugate structure. These results show that the exocyclic double bond could effectively enhance the interaction between the compounds and Topo I by π - π stacking interactions, the π -lone pair stacking interaction and π -alkyl stacking interaction, most likely through strengthening the conjugative effect of the furanone ring of series **2**. The docking results suggest that introduction of a double bond into the furanone ring may be a feasible strategy for the further development Topo I inhibitors.

[Figure 4]

3.2. Cytotoxicity

The MTT assay was used to evaluate antitumor activity by testing the cytotoxicity against three human cancer cells lines, MCF-7 (human breast adenocarcinoma cell line), HeLa (human cervix tumor cell line), A549 (adenocarcinomic human alveolar basal epithelial cell line). Camptothecin (CPT) was again used as a positive control. The cell growth inhibition activities (IC_{50}) of the tested compounds are shown in **Table 2** which shows that the results of cytotoxicity are generally consistent with the inhibitory activity. Compounds **B-3**, **B-5**, **B-8**, **B-12**, **B-13**, **B-15** exhibit higher cytotoxicity than CPT against MCF-7 cells and HeLa cells. Furthermore, **B-15** with the highest antiproliferative activity, is the most active against all three human cancer cell lines. Consistent with the Topo I inhibitory results, compounds of series **1**, lacking the exocyclic double bond, also generally showed poor inhibitory activity. These results demonstrate that 4-(4-substituted amidobenzyl)-furan-2(5H)-one derivatives exhibit positive antitumor activity, probably due, in part to their Topo I inhibitory activity.

[Table 2]

3.3. DNA-insertion assay

Since the results of the Topo I inhibition assay clearly indicate that Topo I is a target of the 4-(4-substituted amidobenzyl)furan-2(5H)-one derivatives, the mechanism of action of these derivatives was investigated. According to the catalytic process of Topo I (**Fig. 5**), the mechanism of inhibition of Topo I possibly consists of insertion into DNA, forming a drug-enzyme-DNA ternary complex, covalent or noncovalent, and retarding the combination between enzyme and DNA [7,26]. Thus, the DNA-insertion assay was performed to confirm whether these compounds can insert into DNA. Ethidium bromide (EB), a DNA intercalating agent, was used as a positive control [27] and CPT, which inhibits Topo I by forming the drug-enzyme-DNA covalent ternary complex, was used as a negative control. As shown in **Fig. 6**, as a DNA-inserting agent, EB can successfully inhibit the conversion of the supercoiled form (lower bands) to the relaxed form (upper bands) in the presence of a large excess of Topo I. However, all of our compounds showed no unwinding effect on DNA even at levels up to 100 μM , and thus are similar to the negative control CPT. This result demonstrates that these furanone derivatives fail to exert Topo I inhibitory activity through DNA insertion.

[Figure 5]

[Figure 6]

3.4. Topo I-mediated DNA cleavage assay

The Topo I-mediated DNA cleavage assay was conducted to investigate whether **B-15**, the most active compound towards Topo I, can stabilize the Topo I-DNA cleavage complex through formation of a drug-enzyme-DNA covalent ternary complex. CPT, which has been shown to stabilize Topo I-cleavable complexes [28], was used as a positive control and the percentage of nicked DNA is shown in **Fig. 7B**. In this assay, Topo I was hydrolyzed by proteinase K, and a secondary electrophoresis was applied to separate the relaxed DNA from nicked DNA. As presented in **Fig. 7**, when treated with 25 μM and 50 μM CPT, the amount of linear DNA was distinctly

increased, as expected. When Topo I was incubated with 25, 50, 100, 200, 400 μM of **B-15**, the percentage of nicked DNA was increased linearly in a concentration-dependent manner. These results indicate that similar to CPT, one of the Topo I inhibitory compounds stabilizes the Topo I-DNA cleavage complex.

[Figure 7]

3.5. Inhibition of the combination between DNA and Topo I

In order to investigate whether **B-15** can also interfere with the binding between Topo I and DNA, an electrophoretic mobility shift assay (EMSA) was performed [29]. In this assay, CPT, which does not inhibit of the binding of Topo I to DNA, was used as a negative control. The proportion of Topo I-DNA complex formed was used to explain the result of the electrophoretic mobility shift assay (**Fig. 8B**). As shown in **Fig. 8**, when treated with 50 and 100 μM of CPT, the amount of Topo I-DNA complex (the middle bands) was generated at a similar level as in the control (Lane B). However, when treated with 50, 100, 200, 300, 400 μM of **B-15**, the percentage of Topo I-DNA complex (the middle bands) diminished linearly in a concentration-dependent manner. These EMSA results clearly indicate that another Topo I inhibitory mechanism of our compound is interfering with the binding of Topo I to DNA.

[Figure 8]

3.6. Molecular docking

The mechanism studies above indicated that our compounds not only can stabilize the drug-enzyme-DNA covalent ternary complex, but also interfere with the binding between Topo I and DNA. Molecular docking studies were carried out in an attempt to confirm this dual action mechanism. The average minimized complex of representative compound **B-15** with Topo I (validated by MD simulation for 20 ns, **Figure S2**), whose maximum free energy (ΔG) calculated by MM-PBSA were -29.7 kcal/mol, was used for binding mode analysis. Firstly, as shown in **Fig. 9**, **B-15** could fit well into the Topo I-DNA covalent complex by interacting not only with amino

acid residues, but also with DNA bases in the active pocket of Topo I. Specifically, the O of amido bond and the lactonic O of furanone ring of **B-15** binds well with residue ARG364 and ASN722 respectively by forming hydrogen bonds (shown as green dashed lines). Meanwhile, the N-H of amido bond of **B-15** forms hydrogen bonds with the DNA base DA113. In addition, the fluorine atom in the para-position can form a strong hydrogen-halogen bond of $-5.5 \text{ kcal} \cdot \text{mol}^{-1}$ with ASN722, while such interaction cannot be observed in the complex of compounds **B-13** and **B-14** (nearly identical with **B-15** except for the substituted fluorine atom attached to the different position on the terminal phenyl ring). As shown in **Figure 10**, lack of this hydrogen-halogen change the whole binding mode, of which the furan ring is bending over, which can provide one possible explanation for the significant potency of **B-15** superior to both **B-13** and **B-14**. As shown in **Fig. 9B**, the π - π stacking interactions (shown as red dashed lines) can be observed between the aromatic ring of **B-15** and amino acid residue TGP11 as well as the DNA bases DA113, DC112 and DT10. Moreover, the furanone ring of **B-15** forms with the amino acid residue LYS425 by the π -alkyl stacking interaction (blue dashed lines). These effective interactions between **B-15** and the Topo I-DNA covalent complex are evidence for the mechanism of stabilization of the drug-enzyme-DNA covalent 4-(4-substituted amidobenzyl)furan-2(5H)-one derivatives.

Since the mechanism studies also reveal that 4-(4-substituted amidobenzyl)furan-2(5H)-one derivatives apparently interfere with the binding of Topo I to DNA, we further docked **B-15** into the 3-dimensional crystal structure of Topo I (PDB: 1K4T), from which the DNA was removed. As shown in **Fig. 9C**, **B-15** also interacts well with the active pocket of DNA-free Topo I by forming hydrogen bonds (showed as yellow dashed lines) with different amino acid residues (HIS367, LYS425, LYS493, ALA499). The results provide evidence for the second mechanism with which these compounds interfere with the binding between Topo I and DNA.

[Figure 9]

[Figure 10]

4. Conclusion

In this study, two series of novel 4-(4-substituted amidobenzyl)furan-2(5H)-one derivatives bearing an α,β -unsaturated lactone moiety, a pharmacophore with potential antitumor activity [9], were designed, synthesized and evaluated for Topo I inhibitory activity and cytotoxicity against three human cancer cell lines. Among the synthetic 4-(4-substituted amidobenzyl)furan-2(5H)-one derivatives, series **2** with an exocyclic double bond, exhibited promising Topo I inhibitory activity and cytotoxicity against cancer cell lines. This suggests that introduction of the exocyclic double bond into the α,β -unsaturated lactones 2-furanone moiety is essential to develop 4-(4-substituted amidobenzyl)furan-2(5H)-one derivatives as Topo I-based antitumor agents. In series **2**, several compounds showing promising activity as Topo I inhibitors and cytotoxicity, especially **B-15**, were identified. Some design principles derived from the binding patterns of this type of compound with Topo I as well as the structure-activity relationships have been summarized, and may be useful in the future to guide the design and modification of new furanone derivatives as Topo I inhibitors. A series of mechanism studies indicate that our compounds can not only stabilize the drug-enzyme-DNA covalent ternary complex but can also interfere with the binding of Topo I to DNA. In the future, we will attempt to develop more potent Topo I inhibitors.

5. Experimental section

5.1. Chemistry

All chemicals were purchased from Alfa Aesar or Sigma Aldrich. The synthetic routes to two series of 4-(4-substituted amidobenzyl)furan-2(5H)-one derivatives are shown in **Scheme 1** and **Scheme 2**. All the compounds were fully identified through ^1H and ^{13}C -nuclear magnetic resonance (NMR), mass spectrometry (MS) and high resolution mass spectrometry (ESI-HRMS). Melting points were determined with a digital melting point apparatus and are uncorrected.

5.1.1. Intermediate compounds **1-1~1-4** and **2-1~2-4**

5.1.1.1.

(E)-3-Benzyl-4-oxobut-2-enoic acid (**1-1**). Glyoxylic acid monohydrate (0.037 mol, 2.76 g) was dissolved in 50 mL of MeOH, and KOH (0.037 mol, 2.08 g) was added to the solution at 0 °C under nitrogen followed by dropwise addition of phenylpropyl aldehyde (0.037 mol, 5 g). The mixture kept overnight at room temperature. The solvent and excess phenylpropyl aldehyde were then removed under reduced pressure, and the residue was diluted with 30 mL of H₂O, and the mixture was extracted with EtOAc (3 × 30 mL). The aqueous phase was acidified with 10% HCl to pH 3 and then extracted with EtOAc (3 × 50 mL). The organic layer was dried over anhydrous Na₂SO₄, filtered concentrated to dryness and purified through a silica gel column (EA: PE: AcOH = 5: 1: 5%) to give *(Z)*-3-benzyl-4-oxobut-2-enoic acid (**1-1**) as a white solid, mp 149.3-150.0 °C, yield 65%; ¹H NMR (300 MHz, CDCl₃) δ 9.59 (s, 1H, -CHO), 7.32 – 7.16 (m, 5H, Ar-H), 6.61 (s, 1H, -C=CH), 4.14 (s, 2H, benzylic CH₂); ¹³C NMR (75 MHz, CDCl₃) δ 193.97 (-CHO), 170.85 (-COOH), 154.32, 137.33, 134.18, 129.18, 128.65, 126.79, 30.46 (benzylic CH₂); ESI-HRMS *m/z*: 189.0559 [M+H]⁺, calcd for C₁₁H₉O₃ 189.0557.

5.1.1.2.

(E)-3-Formyl-4-(4-nitrophenyl)but-2-enoic acid (**1-2**). *(Z)*-3-benzyl-4-oxobut-2-enoic acid (**1-1**, 1.29 mmol, 193 mg) was added portion-wise into stirred nitrosonitric acid (1 mL, 23.80 mmol) at -10 °C. After 4 h, 20 mL of ice was added into the solution and the mixture was stirred for 30 min. The mixture was extracted with EtOAc (3 × 20 mL). The organic layer was dried over anhydrous Na₂SO₄, filtered and concentrated to dryness, then purified through silica gel column (EA: PE: AcOH = 2: 1: 5%) to give *(E)*-3-formyl-4-(4-nitrophenyl)but-2-enoic acid as a yellow solid, mp 176.6-177.6 °C, yield 56%; ¹H NMR (300 MHz, acetone-*d*₆) δ 9.69 (s, 1H, aldehydic), 8.12 (d, *J* = 8.7 Hz, 2H, Ar-H), 7.54 (d, *J* = 8.7 Hz, 2H, Ar-H), 6.94 (s, 1H, -C=CH), 4.18 (s, 2H, benzylic CH₂); ¹³C NMR (75 MHz, Acetone-*d*₆) δ 194.52 (-CHO), 165.93 (-COOH), 150.55, 146.61, 146.38, 137.38, 129.93, 123.27, 29.64 (benzylic CH₂); ESI-HRMS *m/z*: 234.0410 [M-H]⁻, calcd for C₁₁H₈NO₅ 234.0408.

5.1.1.3.

(E)-4-Hydroxy-3-(4-nitrobenzyl)but-2-enoic acid (**1-3**). Compound **1-2** (0.51 mmol, 120 mg) was added into a flask, and 5 mL MeOH was added to the flask at room temperature. Sodium borohydride (2.04 mmol, 80 mg) was added portion-wise to the rapidly stirred reaction mixture. After 2 h, 20 mL of 10 % HCl was added into the solution. The mixture was extracted with EtOAc (3 × 20 mL). The organic layer was dried over anhydrous Na₂SO₄, filtered and concentrated to dryness, which was purified through silica gel column (EA: PE: AcOH = 2: 1: 5%) to give *(E)*-4-hydroxy-3-(4-nitrobenzyl)but-2-enoic acid as a white solid, mp 165.4-166.3 °C, yield 78%; ¹H NMR (300 MHz, DMSO-*d*₆) δ 8.60 (d, *J* = 8.7 Hz, 2H, Ar-H), 8.01 (d, *J* = 8.7 Hz, 2H, Ar-H), 6.69 (s, 1H, -C=CH), 4.61 (s, 2H, -CH₂-OH), 4.57 (d, *J* = 1.6 Hz, 2H, benzylic CH₂); ¹³C NMR (75 MHz, DMSO-*d*₆) δ 167.51 (-COOH), 159.57, 147.71, 130.24, 123.83, 115.29, 64.39 (-CH₂-OH), 34.30 (benzylic CH₂); ESI-HRMS *m/z*: 236.056 [M-H], calcd for C₁₁H₉NO₅ 236.0564.

5.1.1.4.

4-(4-Nitrobenzyl)furan-2(5H)-one (**1-4**). Compound **1-3** (0.61 mmol, 145 mg) and *N*-(3-dimethylaminopropyl)-*N'*-ethylcarbodiimide hydrochloride (0.92 mmol, 176 mg) were placed in a dry double-neck flask, and 5 ml of dry DCM and 0.17 mL of triethylamine (1.23 mmol) were added to the flask under nitrogen separately. The mixture was reacted for 2 h at room temperature then was washed with saturated sodium bicarbonate solution. The organic layer dried over anhydrous Na₂SO₄, filtered and concentrated to dryness, and then purified through a silica gel column (EA: PE = 5: 1) to give 4-(4-nitrobenzyl)furan-2(5H)-one as a white solid, mp 140.0-140.9 °C, yield 72%; ¹H NMR (300 MHz, DMSO-*d*₆) δ 8.19 (d, *J* = 8.7 Hz, 2H, Ar-H), 7.57 (d, *J* = 8.7 Hz, 2H, Ar-H), 5.82 – 5.78 (m, 1H, -C=CH), 4.87 (d, *J* = 1.7 Hz, 2H, -O-CH₂), 3.96 (s, 2H, benzylic CH₂); ¹³C NMR (75 MHz, DMSO-*d*₆) δ 173.28 (carbonyl), 169.88, 146.55, 144.67, 130.35, 123.80, 115.57, 72.80 (-O-CH₂), 33.77 (benzylic CH₂); ESI-HRMS *m/z*: 220.0612 [M+H]⁺, calcd for C₁₁H₁₀NO₄ 220.0604.

5.1.1.5.

4-(4-Nitrophenyl)butan-2-one (**2-1**). 4-Nitrobenzyl bromide (0.2 mol, 42.8 g) and 2,4-pentanedione (0.2 mol, 20 g) were placed a double-neck flask, and 300 mL of

MeOH was added to the flask. When these were completely dissolved, 27.6 g of potassium carbonate was added and the mixture was refluxed for 4 h. When the reaction solution temperature cooled to room temperature, the solvent was removed under reduced pressure, and then 200 mL of H₂O was added. The mixture was extracted with EtOAc (3 × 200 mL), and then the organic layer was dried over anhydrous Na₂SO₄, filtered and concentrated to dryness, and purified through silica gel column (EA: PE = 10: 1) to give 4-(4-nitrophenyl)butan-2-one as white crystals, mp 56.1-57.0 °C, yield 66%; ¹H NMR (300 MHz, CDCl₃) δ 8.08 (d, *J* = 8.7 Hz, 2H, Ar-H), 7.32 (d, *J* = 8.7 Hz, 2H, Ar-H), 2.96 (t, *J* = 7.3 Hz, 2H, benzylic CH₂), 2.79 (t, *J* = 7.2 Hz, 2H, -CO-CH₂), 2.13 (s, 3H, -CO-CH₃); ¹³C NMR (75 MHz, CDCl₃) δ 206.83 (carbonyl), 149.09, 146.45, 129.31, 123.71, 44.14 (benzylic CH₂), 30.06 (-CO-CH₂), 29.33 (-CO-CH₃); ESI-HRMS *m/z*: 194.0814 [M+H]⁺, calcd for C₁₀H₁₂NO₃ 194.0812.

5.1.1.6.

(*E*)-3-(4-Nitrobenzyl)-4-oxopent-2-enoic acid (**2-2**). Compound **2-1** (128.20 mmol, 25 g) and glyoxylic acid monohydrate (270.27 mmol, 20 g) were added into a double-neck flask, and 100 mL of phosphoric acid was added to the flask. The mixture was refluxed for 4 h. When the reaction solution temperature cooled to room temperature, 200 mL of H₂O was added. The mixture was extracted with EtOAc (3 × 200 mL), and the organic layer was extracted with 30% K₂CO₃ (3 × 150 mL). The aqueous phase was acidified with 10% hydrochloric acid to pH 3 and then extracted with EtOAc (3 × 100 mL). The organic layer was dried over anhydrous Na₂SO₄, filtered and concentrated to dryness, then purified through a silica gel column (CH₂Cl₂: MeOH = 200: 1) to give (*E*)-3-(4-nitrobenzyl)-4-oxopent-2-enoic acid as a yellow solid, mp 177.6-178.5 °C, yield 72%; ¹H NMR (300 MHz, CDCl₃) δ 8.10 (d, *J* = 8.7 Hz, 2H, Ar-H), 7.40 (d, *J* = 8.7 Hz, 2H, Ar-H), 6.78 (s, 1H, -C=CH), 4.27 (s, 2H, benzylic CH₂), 2.40 (s, 3H, -CO -CH₃); ¹³C NMR (75 MHz, CDCl₃) δ 198.78 (carbonyl), 170.30 (-COOH), 153.31, 146.71, 145.99, 129.91, 127.30, 123.78, 31.85 (benzylic CH₂), 26.68 (-CO-CH₃); ESI-HRMS *m/z*: 248.0561 [M-H]⁻, calcd for C₁₂H₁₀NO₅ 248.0564.

5.1.1.7.

5-Methylene-4-(4-nitrobenzyl)furan-2(5H)-one (2-3). Compound **2-2** (0.28 mol, 70 g) and *p*-toluenesulfonic acid (0.84 mol, 159.6 g) was added into a double-neck flask, and 400 mL of toluene was added to the flask. The mixture was refluxed for 6 h. When the reaction solution temperature cooled to room temperature, the solvent was removed under reduced pressure, and then 400 mL of H₂O was added. The mixture was extracted with EtOAc (3 × 200 mL). The organic layer was dried over anhydrous Na₂SO₄, filtered and concentrated to dryness, and purified through a silica gel column (EA: PE = 5: 1) to give 5-methylene-4-(4-nitrobenzyl)furan-2(5H)-one as a yellow solid, mp 136.7-137.6 °C, yield 45%; ¹H NMR (300 MHz, CDCl₃) δ 8.23 (d, *J* = 8.7 Hz, 2H, Ar-H), 7.40 (d, *J* = 8.7 Hz, 2H, Ar-H), 5.87 (d, *J* = 0.9 Hz, 1H, -C=CH), 5.24 (dd, *J* = 3.1, 1.8 Hz, 1H, exocyclic -C=CH), 4.93 (dd, *J* = 3.1, 0.7 Hz, 1H, exocyclic -C=CH), 3.94 (s, 2H, benzylic CH₂); ¹³C NMR (75 MHz, CDCl₃) δ 168.20 (-CO), 155.88, 155.23, 147.45, 143.37, 129.83, 124.40, 119.25, 95.55 (exocyclic -C=CH), 32.44 (benzylic CH₂); ESI-HRMS *m/z*: 232.0612 [M+H]⁺, calcd for C₁₂H₁₀NO₄ 232.0604.

5.1.1.8.

4-(4-Aminobenzyl)-5-methylenefuran-2(5H)-one (2-4). Compound **2-3** (10 mmol, 2.5 g), ammonium chloride (10 mmol, 532 mg) and Fe (30 mmol, 1.67 g) were placed in a double-neck flask, and 40 mL of THF and 8 mL of H₂O were added to the flask. The mixture was refluxed under nitrogen for 4 h. When the reaction solution temperature cooled to room temperature, 20 mL of H₂O was added. The excess of Fe was filtered, and the mixture was extracted with EtOAc (3 × 20 mL). The organic layer was dried over anhydrous Na₂SO₄, filtered and concentrated to dryness, then was purified through silica gel column (EA: PE = 5: 1) to give 4-(4-aminobenzyl)-5-methylene-furan-2(5H)-one as a yellow oil, yield 67%; ¹H NMR (300 MHz, CDCl₃) δ 6.95 (d, *J* = 8.4 Hz, 2H, Ar-H), 6.63 (d, *J* = 8.4 Hz, 2H, Ar-H), 5.80 (d, *J* = 0.9 Hz, 1H, -C=CH), 5.14 (dd, *J* = 2.8, 1.8 Hz, 1H, exocyclic -C=CH), 4.93 (dd, *J* = 2.9, 0.6 Hz, 1H, exocyclic -C=CH), 3.66 (d, *J* = 1.1 Hz, 2H, benzylic CH₂); ¹³C NMR (75 MHz, CDCl₃) δ 169.01 (-CO), 159.03, 155.53, 145.67,

129.61, 125.41, 117.99, 115.44, 94.96 (exocyclic -C=CH), 31.83 (benzylic CH₂); ESI-HRMS *m/z*: 202.0854 [M+H]⁺, calcd for C₁₂H₁₂NO₃ 202.0863.

5.1.2. General procedure of the preparation of **A-1~A-7**

Compound **1-4** (10 mmol, 2.5 g), ammonium chloride (10 mmol, 532 mg) and Fe (30 mmol, 1.67 g) were placed in a double-neck flask, and 40 mL of THF and 8 mL of H₂O were added to the flask. The mixture was refluxed under nitrogen for 4 h. When the reaction solution temperature cooled to room temperature, 20 mL of H₂O was added. The excess of Fe was filtered, and the mixture was extracted with EtOAc (3 × 20 mL). The organic layer was dried over anhydrous Na₂SO₄, filtered and concentrated to obtain the intermediate aminofuranone, which was used in the next reaction without purification. The carboxylic acid (0.75 mmol) was added into a dry double-neck flask, and 5 mL of dry THF was added to the flask. *N,N*-Dimethylformamide (1.50 mmol, 0.15 mL) was added into the solution under nitrogen at 0 °C. When these were completely dissolved, oxalyl chloride (3.75 mmol) was added slowly. After 30 min, the solvent and excess oxalyl chloride were then removed under reduced pressure to obtain an acyl chloride. The acyl chloride was kept dry. 100 mg of the intermediate amino furanone was added into a dry double-neck flask, and 5 mL of dry THF was added to the flask. When these were completely dissolved, dry pyridine (1.06 mmol, 0.01 mL) was added under nitrogen at 0 °C. The THF solution of an acyl chloride (0.793 mmol) was added into the mixture slowly. After 30 min, 20 mL of saturated ammonium chloride solution was slowly added into the mixture, and the mixture was extracted three times with EtOAc (3 × 20 mL). The organic layer was dried over anhydrous Na₂SO₄, filtered and concentrated to dryness, which was purified through silica gel column (EA: PE = 2: 1) to give **A-1~A-7**.

5.1.2.1.

N-(4-((5-Oxo-2,5-dihydrofuran-3-yl)methyl)phenyl)-2-(*p*-tolyl)acetamide (**A-1**)

White solid, mp 105.5-106.4 °C, yield 78%; ¹H NMR (300 MHz, Acetone-*d*₆) δ 9.31 (s, 1H, N-H), 7.63 (d, *J* = 8.4 Hz, 2H, Ar-H), 7.23 (dd, *J* = 15.3, 8.1 Hz, 4H, Ar-H), 7.12 (d, *J* = 8.4 Hz, 2H, Ar-H), 5.73 (s, 1H, -C=CH), 4.79 (s, 2H, -O-CH₂), 3.78 (s,

2H, benzylic CH₂), 3.63 (s, 2H, benzylic CH₂), 2.28 (s, 3H, Ar-CH₃); ¹³C NMR (75 MHz, Acetone-*d*₆) δ 173.99 (-CO), 171.59 (-CO), 170.03, 139.32, 136.87, 133.76, 132.37, 130.06, 129.90, 129.81, 120.39, 116.15, 73.34 (-O-CH₂), 44.34 (benzylic CH₂), 34.76 (benzylic CH₂), 21.02 (Ar-CH₃); ESI-MS *m/z*: 322.1 [M+H]⁺; ESI-HRMS *m/z*: 322.1450 [M+H]⁺, calcd for C₂₀H₂₀NO₃ 322.1438.

5.1.2.2.

N-(4-((5-Oxo-2,5-dihydrofuran-3-yl)methyl)phenyl)-2-(2-(trifluoromethyl)phenyl)acetamide (**A-2**). White solid, mp 127.8-128.3 °C, yield 55%; ¹H NMR (300 MHz, Acetone-*d*₆) δ 9.44 (s, 1H, N-H), 7.73 (d, *J* = 7.8 Hz, 1H, Ar-H), 7.68 – 7.56 (m, 4H, Ar-H), 7.49 (t, *J* = 7.5 Hz, 1H, Ar-H), 7.24 (d, *J* = 8.4 Hz, 2H, Ar-H), 5.78 – 5.73 (m, 1H, -C=CH), 4.81 (d, *J* = 1.6 Hz, 2H, -O-CH₂), 3.98 (s, 2H, benzylic CH₂), 3.81 (s, 2H, benzylic CH₂); ¹³C NMR (75 MHz, Acetone-*d*₆) δ 173.17 (-CO), 170.71 (-CO), 167.81, 138.31, 134.05, 133.30, 132.04, 131.65, 129.25, 127.22, 126.56, 125.65, 122.49, 119.64, 115.32, 72.50 (-O-CH₂), 40.03 (benzylic CH₂), 33.90 (benzylic CH₂); ESI-MS *m/z*: 376.3 [M+H]⁺; ESI-HRMS *m/z*: 376.1160 [M+H]⁺, calcd for C₂₀H₁₇FNO₃ 376.1155.

5.1.2.3.

N-(4-((5-Oxo-2,5-dihydrofuran-3-yl)methyl)phenyl)-2-(3-(trifluoromethyl)phenyl)acetamide (**A-3**). White solid, mp 126.6-127.2 °C, yield 51%; ¹H NMR (300 MHz, Acetone-*d*₆) δ 9.47 (s, 1H, N-H), 7.73 (s, 1H, Ar-H), 7.70 – 7.51 (m, 5H, Ar-H), 7.22 (d, *J* = 8.5 Hz, 2H, Ar-H), 5.75 – 5.66 (m, 1H, -C=CH), 4.79 (d, *J* = 1.7 Hz, 2H, -O-CH₂), 3.84 (s, 2H, benzylic CH₂), 3.79 (s, 2H, benzylic CH₂); ¹³C NMR (75 MHz, Acetone-*d*₆) δ 174.00 (-CO), 171.54 (-CO), 169.17, 139.13, 138.19, 134.15, 132.63, 130.84, 130.14, 130.02, 126.84, 125.36, 124.28, 120.51, 116.21, 73.37 (-O-CH₂), 44.00 (benzylic CH₂), 34.78 (benzylic CH₂); ESI-MS *m/z*: 376.2 [M+H]⁺; ESI-HRMS *m/z*: 376.1158 [M+H]⁺, calcd for C₂₀H₁₇FNO₃ 376.1155.

5.1.2.4.

N-(4-((5-Oxo-2,5-dihydrofuran-3-yl)methyl)phenyl)-2-(4-(trifluoromethyl)phenyl)acetamide (**A-4**). White solid, mp 139.8-140.7 °C, yield 66%; ¹H NMR (300 MHz, Acetone-*d*₆) δ 9.46 (s, 1H, N-H), 7.75 – 7.51 (m, 6H, Ar-H), 7.22 (d, *J* = 8.4 Hz, 2H,

Ar-H), 5.79 – 5.64 (m, 1H, -C=CH), 4.79 (d, $J = 1.7$ Hz, 2H, -O-CH₂), 3.83 (s, 2H, benzylic CH₂), 3.79 (s, 2H, benzylic CH₂); ¹³C NMR (75 MHz, Acetone-*d*₆) δ 174.00 (-CO), 171.54 (-CO), 169.05, 141.50, 139.12, 135.27, 132.65, 130.92, 130.13, 125.98, 125.46, 120.53, 116.21, 73.37 (-O-CH₂), 44.20 (benzylic CH₂), 34.78 (benzylic CH₂); ESI-MS m/z : 376.2 [M+H]⁺; ESI-HRMS m/z : 376.1146 [M+H]⁺, calcd for C₂₀H₁₇FNO₃ 376.1155.

5.1.2.5.

(*E*)-3-(2-Fluorophenyl)-*N*-(4-((5-oxo-2,5-dihydrofuran-3-yl)methyl)phenyl)acrylamide (**A-5**). Yellow solid, mp 154.0-155.0 °C, yield 65%; ¹H NMR (300 MHz, Acetone-*d*₆) δ 9.57 (s, 1H, N-H), 7.83 – 7.75 (m, 3H, Ar-H, -C=CH), 7.67 (dd, $J = 10.8, 4.6$ Hz, 1H, Ar-H), 7.49 – 7.39 (m, 1H, Ar-H), 7.31 – 7.15 (m, 4H, Ar-H), 6.96 (d, $J = 15.8$ Hz, 1H, -C=CH), 5.85 – 5.65 (m, 1H, -C=CH), 4.82 (d, $J = 1.1$ Hz, 2H, -O-CH₂), 3.82 (s, 2H, benzylic CH₂); ¹³C NMR (75 MHz, Acetone-*d*₆) δ 174.05 (-CO), 171.57, 164.29 (-CO), 162.04, 139.27, 139.14, 134.10, 132.72, 132.28, 130.19, 125.67, 125.62, 123.70, 120.63, 117.00, 116.86, 73.40 (-O-CH₂), 34.82 (benzylic CH₂); ESI-MS m/z : 338.1 [M+H]⁺; ESI-HRMS m/z : 338.1191 [M+H]⁺, calcd for C₂₀H₁₇FNO₃ 338.1187.

5.1.2.6.

(*E*)-3-(3-Fluorophenyl)-*N*-(4-((5-oxo-2,5-dihydrofuran-3-yl)methyl)phenyl)acrylamide (**A-6**). Yellow solid, mp 155.6-156.3 °C, yield 61%; ¹H NMR (300 MHz, Acetone-*d*₆) δ 9.55 (s, 1H, N-H), 7.77 (d, $J = 8.5$ Hz, 2H, Ar-H), 7.67 (d, $J = 15.6$ Hz, 1H, -C=CH), 7.44 (m, 2H, Ar-H), 7.37 (d, $J = 10.5$ Hz, 1H, Ar-H), 7.26 (d, $J = 8.5$ Hz, 2H, Ar-H), 7.20 – 7.10 (m, 1H, Ar-H), 6.90 (d, $J = 15.6$ Hz, 1H, -C=CH), 5.79 – 5.73 (m, 1H, -C=CH), 4.82 (d, $J = 1.3$ Hz, 2H, -O-CH₂), 3.81 (s, 2H, benzylic CH₂); ¹³C NMR (75 MHz, Acetone-*d*₆) δ 174.10 (-CO), 171.60, 164.20 (-CO), 163.85, 140.27, 139.20, 138.52, 132.72, 131.63, 130.18, 124.84, 124.44, 120.65, 117.11, 116.20, 114.69, 73.41 (-O-CH₂), 34.80 (benzylic CH₂); ESI-MS m/z : 338.4 [M+H]⁺; ESI-HRMS m/z : 338.1200 [M+H]⁺, calcd for C₂₀H₁₇FNO₃ 338.1187.

5.1.2.7.

(*E*)-3-(4-Fluorophenyl)-*N*-(4-((5-oxo-2,5-dihydrofuran-3-yl)methyl)phenyl)acrylamide (**A-7**). White solid, mp 182.1-183.0 °C, yield 71%; ¹H NMR (300 MHz, Acetone-*d*₆) δ 9.45 (s, 1H, N-H), 7.76 (d, *J* = 8.5 Hz, 2H, Ar-H), 7.70-7.64 (m, 3H, Ar-H, -C=CH), 7.26 (d, *J* = 8.5 Hz, 2H, Ar-H), 7.19 (t, *J* = 8.8 Hz, 2H, Ar-H), 6.80 (d, *J* = 15.6 Hz, 1H, -C=CH), 5.77 – 5.74 (m, 1H, -C=CH), 4.82 (d, *J* = 1.7 Hz, 2H, -O-CH₂), 3.83 (s, 2H, benzylic CH₂); ¹³C NMR (75 MHz, Acetone-*d*₆) δ 173.12 (-CO), 170.70, 165.11 (-CO), 163.47, 139.51, 138.49, 131.71, 131.65, 129.87, 129.32, 121.93, 119.66, 115.80, 115.34, 72.50 (-O-CH₂), 33.95 (benzylic CH₂); ESI-MS *m/z*: 338.2 [M+H]⁺; ESI-HRMS *m/z*: 338.1199 [M+H]⁺, calcd for C₂₀H₁₇FNO₃ 338.1187.

5.1.3. General procedure for the preparation of **B-1~B-15**

A carboxylic acid (0.75 mmol) was added into a dry double-neck flask, and 5 mL of dry THF was added to the flask. *N,N*-dimethylformamide (1.50 mmol, 0.15 mL) was added into the solution under nitrogen at 0 °C. When the solids were completely dissolved, oxalyl chloride (3.75 mmol) was added slowly. After 30 min, the solvent and excess oxalyl chloride were removed under reduced pressure to obtain an acyl chloride which was kept dry. 100 mg of compound **2-4** (0.53 mmol) was added into a dry double-neck flask, and 5 mL of dry THF was added to the flask. When these were completely dissolved, dry pyridine (1.06 mmol, 0.01 mL) was added under nitrogen at 0 °C. The THF solution of an acyl chloride (0.793 mmol) was added into the mixture slowly. After 30 min, 20 mL of saturated ammonium chloride solution was slowly added into the mixture, and the mixture was extracted with EtOAc (3 × 20 mL). The organic layer was dried over anhydrous Na₂SO₄, filtered and concentrated to dryness, then purified through silica gel column (EA: PE = 2: 1) to give **B-1~B-15**.

5.1.3.1.

N-(4-((2-Methylene-5-oxo-2,5-dihydrofuran-3-yl)methyl)phenyl)benzamide (**B-1**).

Yellow oil, yield 67%; ¹H NMR (300 MHz, Acetone-*d*₆) δ 9.59 (s, 1H, N-H), 7.99 (d, *J* = 8.5 Hz, 2H, Ar-H), 7.85 (d, *J* = 8.5 Hz, 2H, Ar-H), 7.47 – 7.56 (m, 3H, Ar-H), 7.32 (d, *J* = 8.5 Hz, 2H, Ar-H), 6.02 (s, 1H, -C=CH), 5.16 - 5.19 (m, 2H, exocyclic -C=CH₂), 3.94 (s, 2H, benzylic CH₂); ¹³C NMR (75 MHz, Acetone-*d*₆) δ 168.23

(-CO), 165.50 (-CO), 158.71, 155.68, 138.38, 135.36, 132.19, 131.49, 129.16, 128.41, 127.45, 120.48, 117.85, 94.44 (exocyclic -C=CH₂), 31.44 (benzylic CH₂); ESI-MS *m/z*: 306.3 [M+H]⁺; ESI-HRMS *m/z*: 306.1142 [M+H]⁺, calcd for C₁₉H₁₆NO₃ 306.1125.

5.1.3.2.

N-(4-((2-Methylene-5-oxo-2,5-dihydrofuran-3-yl)methyl)phenyl)-2-phenylacetamide (**B-2**). Yellow oil, yield 71%; ¹H NMR (300 MHz, Acetone-*d*₆) δ 9.38 (s, 1H, N-H), 7.64 (d, *J* = 8.5 Hz, 2H, Ar-H), 7.37 (d, *J* = 7.4 Hz, 2H, Ar-H), 7.33 (s, 1H, Ar-H), 7.30 (d, *J* = 7.4 Hz, 2H, Ar-H), 7.24 (d, *J* = 8.5 Hz, 2H, Ar-H), 5.98 (s, 1H, -C=CH), 5.19 – 5.10 (m, 2H, exocyclic -C=CH₂), 3.89 (s, 2H, benzylic CH₂), 3.68 (s, 2H, benzylic CH₂); ¹³C NMR (75 MHz, Acetone-*d*₆) δ 168.97 (-CO), 168.18 (-CO), 158.71, 155.65, 138.41, 135.98, 131.77, 129.53, 129.16, 128.32, 126.61, 119.52, 117.79, 94.37 (exocyclic -C=CH₂), 43.84 (benzylic CH₂), 31.36 (benzylic CH₂); ESI-MS *m/z*: 320.0 [M+H]⁺; ESI-HRMS *m/z*: 320.1295 [M+H]⁺, calcd for C₂₀H₁₈NO₃ 320.1281.

5.1.3.3.

N-(4-((2-Methylene-5-oxo-2,5-dihydrofuran-3-yl)methyl)phenyl)-2-(*p*-tolyl)acetamide (**B-3**). White solid, mp 119.8-120.7 °C, yield 71%; ¹H NMR (300 MHz, Acetone-*d*₆) δ 9.36 (s, 1H, N-H), 7.64 (d, *J* = 8.5 Hz, 2H, Ar-H), 7.25 (dd, *J* = 8.1, 4.9 Hz, 4H, Ar-H), 7.13 (d, *J* = 8.5 Hz, 2H, Ar-H), 6.00 (s, 1H, -C=CH), 5.13 – 5.18 (m, 2H, exocyclic -C=CH₂), 3.90 (s, 2H, benzylic CH₂), 3.64 (s, 2H, benzylic CH₂), 2.29 (s, 3H, Ar-CH₃); ¹³C NMR (75 MHz, Acetone-*d*₆) δ 169.20 (-CO), 168.19 (-CO), 158.72, 155.66, 138.44, 136.00, 132.89, 131.73, 129.13, 129.04, 128.95, 119.49, 117.73, 94.36 (exocyclic -C=CH₂), 43.47 (benzylic CH₂), 31.36 (benzylic CH₂), 20.17 (Ar-CH₃); ESI-MS *m/z*: 334.1 [M+H]⁺; ESI-HRMS *m/z*: 334.1451 [M+H]⁺, calcd for C₂₁H₂₀NO₃ 334.1438.

5.1.3.4.

N-(4-((2-Methylene-5-oxo-2,5-dihydrofuran-3-yl)methyl)phenyl)-2-(2-(trifluoromethyl)phenyl)acetamide (**B-4**). White solid, mp 124.6-125.5 °C, yield 56%; ¹H NMR (300 MHz, CDCl₃) δ 7.68 (d, *J* = 7.7 Hz, 1H, Ar-H), 7.55-7.50 (m, 2H, Ar-H), 7.44 (d,

$J = 8.3$ Hz, 2H, Ar-H), 7.40 (d, $J = 8.4$ Hz, 1H, Ar-H), 7.10 (d, $J = 8.3$ Hz, 2H, Ar-H), 5.78 (s, 1H, -C=CH), 5.17 – 5.14 (m, 1H, exocyclic -C=CH), 4.92 (d, $J = 2.8$ Hz, 1H, exocyclic -C=CH), 3.88 (s, 2H, benzylic CH₂), 3.74 (s, 2H, benzylic CH₂); ¹³C NMR (75 MHz, CDCl₃) δ 168.94 (-CO), 168.24 (-CO), 158.13, 155.48, 137.03, 132.80, 132.67, 132.43, 131.96, 129.36, 129.12, 127.82, 126.39, 122.62, 120.65, 118.53, 95.30 (exocyclic -C=CH₂), 41.16 (benzylic CH₂), 32.05 (benzylic CH₂); ESI-MS m/z : 388.4 [M+H]⁺; ESI-HRMS m/z : 388.1148 [M+H]⁺, calcd for C₂₁H₁₇F₃NO₃ 388.1155.

5.1.3.5.

N-(4-((2-Methylene-5-oxo-2,5-dihydrofuran-3-yl)methyl)phenyl)-2-(3-(trifluoromethyl)phenyl)acetamide (**B-5**). White solid, mp 115.6-116.3 °C, yield 59%; ¹H NMR (300 MHz, Acetone-*d*₆) δ 9.52 (s, 1H, N-H), δ 7.74 (s, 1H, Ar-H), 7.69 (d, $J = 7.4$, 1H, Ar-H), 7.65 (d, $J = 8.5$ Hz, 2H, Ar-H), 7.60 (d, $J = 3.3$, 1H, Ar-H), 7.56 (d, $J = 7.4$ Hz, 1H, Ar-H), 7.25 (d, $J = 8.5$ Hz, 2H, Ar-H), 5.99 (s, 1H, -C=CH), 5.18 – 5.14 (m, 2H, exocyclic -C=CH₂), 3.90 (s, 2H, benzylic CH₂), 3.84 (s, 2H, benzylic CH₂); ¹³C NMR (75 MHz, Acetone-*d*₆) δ 168.29 (-CO), 168.18 (-CO), 158.67, 155.66, 138.24, 137.31, 133.29, 131.96, 129.94, 129.20, 129.14, 128.08, 125.96, 123.40, 119.59, 117.80, 94.35 (exocyclic -C=CH₂), 43.11 (benzylic CH₂), 31.36 (benzylic CH₂); ESI-MS m/z : 386.2 [M-H]; ESI-HRMS m/z : 388.1147 [M+H]⁺, calcd for C₂₁H₁₇F₃NO₃ 388.1155.

5.1.3.6.

N-(4-((2-Methylene-5-oxo-2,5-dihydrofuran-3-yl)methyl)phenyl)-2-(4-(trifluoromethyl)phenyl)acetamide (**B-6**). White solid, mp 145.3-146.3 °C, yield 70%; ¹H NMR (300 MHz, Acetone-*d*₆) δ 9.49 (s, 1H, N-H), 7.69 – 7.58 (m, 6H, Ar-H), 7.26 (d, $J = 8.5$ Hz, 2H, Ar-H), 5.99 (s, 1H, -C=CH), 5.18 – 5.12 (m, 2H, exocyclic -C=CH₂), 3.90 (s, 2H, benzylic CH₂), 3.82 (s, 2H, benzylic CH₂); ¹³C NMR (75 MHz, Acetone-*d*₆) δ 168.17 (-CO), 168.16 (-CO), 158.67, 155.65, 140.58, 138.23, 131.98, 131.35, 130.05, 129.20, 125.10, 122.32, 119.59, 117.80, 94.36 (exocyclic -C=CH₂), 43.31 (benzylic CH₂), 31.36 (benzylic CH₂); ESI-MS m/z : 388.4 [M+H]⁺; ESI-HRMS m/z : 388.1150 [M+H]⁺, calcd for C₂₁H₁₇F₃NO₃ 388.1155.

5.1.3.7.

2-(2-Fluorophenyl)-N-(4-((2-methylene-5-oxo-2,5-dihydrofuran-3-yl)methyl)phenyl)acetamide (B-7). Yellow oil, yield 61%; ^1H NMR (300 MHz, Acetone- d_6) δ 9.42 (s, 1H, N-H), 7.65 (d, $J = 8.5$ Hz, 2H, Ar-H), 7.44 – 7.38 (m, 1H, Ar-H), 7.35-7.29 (m, 1H, Ar-H), 7.27 (d, $J = 8.5$ Hz, 2H, Ar-H), 7.18 – 7.05 (m, 2H, Ar-H), 5.99 (s, 1H, -C=CH), 5.19 – 5.11 (m, 2H, exocyclic -C=CH₂), 3.89 (s, 2H, benzylic CH₂), 3.77 (s, 2H, benzylic CH₂); ^{13}C NMR (75 MHz, Acetone- d_6) δ 168.19 (-CO), 167.89 (-CO), 161.18, 158.70, 155.66, 138.33, 131.94, 131.84, 129.18, 128.78, 124.13, 122.88, 119.57, 117.80, 115.08, 94.44 (exocyclic -C=CH₂), 36.59 (benzylic CH₂), 31.37 (benzylic CH₂); ESI-MS m/z : 338.4 [M+H]⁺; ESI-HRMS m/z : 338.1193 [M+H]⁺, calcd for C₂₀H₁₇FNO₃ 338.1187.

5.1.3.8.

2-(4-Fluorophenyl)-N-(4-((2-methylene-5-oxo-2,5-dihydrofuran-3-yl)methyl)phenyl)acetamide (B-8). White solid, mp 135.1-136.0 °C, yield 75%; ^1H NMR (300 MHz, Acetone- d_6) δ 9.38 (s, 1H, N-H), 7.63 (d, $J = 8.4$ Hz, 2H, Ar-H), 7.40 (dd, $J = 8.2, 5.7$ Hz, 2H, Ar-H), 7.24 (d, $J = 8.4$ Hz, 2H, Ar-H), 7.07 (t, $J = 8.8$ Hz, 2H, Ar-H), 5.98 (s, 1H, -C=CH), 5.20 – 5.07 (m, 2H, exocyclic -C=CH₂), 3.89 (s, 2H, benzylic CH₂), 3.69 (s, 2H, benzylic CH₂); ^{13}C NMR (75 MHz, Acetone- d_6) δ 168.87 (-CO), 168.19 (-CO), 161.79, 158.69, 155.65, 138.33, 132.01, 131.86, 131.02, 129.18, 119.58, 117.79, , 114.91, 94.37 (exocyclic -C=CH₂), 42.77 (benzylic CH₂), 31.37 (benzylic CH₂); ESI-MS m/z : 338.2 [M+H]⁺; ESI-HRMS m/z : 338.1196 [M+H]⁺, calcd for C₂₀H₁₇FNO₃ 338.1187.

5.1.3.9.

2-(2-Chlorophenyl)-N-(4-((2-methylene-5-oxo-2,5-dihydrofuran-3-yl)methyl)phenyl)acetamide (B-9). White solid, mp 122.5-130.5 °C, yield 65%; ^1H NMR (300 MHz, Acetone- d_6) δ 9.41 (s, 1H, N-H), 7.65 (d, $J = 8.4$ Hz, 2H, Ar-H), 7.47 – 7.39 (m, 2H, Ar-H), 7.31 – 7.27 (m, 2H, Ar-H), 7.25 (d, $J = 8.4$, 2H, Ar-H), 6.00 (s, 1H, -C=CH), 5.18 – 5.11 (m, 2H, exocyclic -C=CH₂), 3.89 (s, 2H, benzylic CH₂), 3.87 (s, 2H, benzylic CH₂); ^{13}C NMR (75 MHz, Acetone- d_6) δ 169.04 (-CO), 168.59 (-CO), 159.54, 156.50, 139.18, 135.05, 134.81, 132.94, 132.67, 130.03, 129.96, 129.37, 127.82, 120.43, 118.64, 95.23 (exocyclic -C=CH₂), 42.03 (benzylic CH₂), 32.22

(benzylic CH₂); ESI-MS m/z : 354.3 [M+H]⁺; ESI-HRMS m/z : 354.0897 [M+H]⁺, calcd for C₂₀H₁₇ClNO₃ 354.0891.

5.1.3.10.

2-(3-Chlorophenyl)-N-(4-((2-methylene-5-oxo-2,5-dihydrofuran-3-yl)methyl)phenyl)acetamide (B-10). Yellow solid, mp 128.8-129.5 °C, yield 68%; ¹H NMR (300 MHz, Acetone-*d*₆) δ 9.44 (s, 1H, N-H), 7.63 (d, $J = 8.4$ Hz, 2H, Ar-H), 7.43 (s, 1H, Ar-H), 7.35 – 7.27 (m, 3H, Ar-H), 7.25 (d, $J = 8.4$ Hz, 2H, Ar-H), 5.98 (s, 1H, -C=CH), 5.18 – 5.10 (m, 2H, exocyclic -C=CH₂), 3.89 (s, 2H, benzylic CH₂), 3.72 (s, 2H, benzylic CH₂); ¹³C NMR (75 MHz, Acetone-*d*₆) δ 169.21 (-CO), 169.03 (-CO), 159.53, 156.51, 139.14, 139.11, 134.38, 132.78, 130.78, 130.11, 130.04, 128.67, 127.53, 120.44, 118.65, 95.22 (exocyclic -C=CH₂), 44.01 (benzylic CH₂), 32.22 (benzylic CH₂); ESI-MS m/z : 354.3 [M+H]⁺; ESI-HRMS m/z : 354.0892 [M+H]⁺, calcd for C₂₀H₁₇ClNO₃ 354.0891.

5.1.3.11.

2-(4-Chlorophenyl)-N-(4-((2-methylene-5-oxo-2,5-dihydrofuran-3-yl)methyl)phenyl)acetamide (B-11). White solid, mp 118.7-119.6 °C, yield 72%; ¹H NMR (300 MHz, Acetone-*d*₆) δ 9.41 (s, 1H, N-H), 7.63 (d, $J = 8.4$ Hz, 2H, Ar-H), 7.41 – 7.31 (m, 4H, Ar-H), 7.25 (d, $J = 8.4$ Hz, 2H, Ar-H), 5.98 (s, 1H, -C=CH), 5.19 – 5.11 (m, 2H, exocyclic -C=CH₂), 3.90 (s, 2H, benzylic CH₂), 3.70 (s, 2H, benzylic CH₂); ¹³C NMR (75 MHz, Acetone-*d*₆) δ 169.40 (-CO), 169.03 (-CO), 159.54, 156.52, 139.17, 135.74, 132.90, 132.75, 131.84, 130.03, 129.14, 120.43, 118.66, 95.21 (exocyclic -C=CH₂), 43.76 (benzylic CH₂), 32.23 (benzylic CH₂); ESI-MS m/z : 376.3 [M+Na]⁺; ESI-HRMS m/z : 354.0895 [M+H]⁺, calcd for C₂₀H₁₇ClNO₃ 354.0891.

5.1.3.12.

N-(4-((2-Methylene-5-oxo-2,5-dihydrofuran-3-yl)methyl)phenyl)cinnamamide (B-12). White solid, mp 139.3-140.0 °C, yield 75%; ¹H NMR (300 MHz, Acetone-*d*₆) δ 9.46 (s, 1H, N-H), 7.77 (d, $J = 8.4$ Hz, 2H, Ar-H), 7.68 (d, $J = 15.6$ Hz, 1H, -C=CH), 7.63 – 7.60 (m, 2H, Ar-H), 7.46 – 7.28 (m, 3H, Ar-H), 7.30 (d, $J = 8.4$ Hz, 2H, Ar-H), 6.86 (d, $J = 15.6$ Hz, 1H, -C=CH), 6.02 (s, 1H, -C=CH), 5.20 – 5.14 (m, 2H,

exocyclic -C=CH₂), 3.93 (s, 2H, benzylic CH₂); ¹³C NMR (75 MHz, Acetone-*d*₆) δ 169.10 (-CO), 164.46 (-CO), 159.57, 156.57, 141.65, 139.52, 136.06, 132.78, 130.55, 130.12, 129.79, 128.63, 122.84, 120.41, 118.58, 95.31 (exocyclic -C=CH₂), 32.09 (benzylic CH₂); ESI-MS *m/z*: 332.0 [M+H]⁺; ESI-HRMS *m/z*: 332.1274 [M+H]⁺, calcd for C₂₁H₁₈NO₃ 332.1281.

5.1.3.13.

(*E*)-3-(2-Fluorophenyl)-*N*-(4-((2-methylene-5-oxo-2,5-dihydrofuran-3-yl)methyl)phenyl)acrylamide (**B-13**). White solid, mp 119.7-120.5 °C, yield 73%; ¹H NMR (300 MHz, Acetone-*d*₆) δ 9.57 (s, 1H, N-H), 7.81 – 7.76 (m, 3H, Ar-H, -C=CH), 7.72 – 7.65 (m, 1H, Ar-H), 7.48 – 7.40 (m, 1H, Ar-H), 7.30 (d, *J* = 8.5 Hz, 2H, Ar-H), 7.27 – 7.17 (m, 2H, Ar-H), 6.96 (d, *J* = 15.6 Hz, 1H, -C=CH), 6.02 (s, 1H, -C=CH), 5.20 – 5.14 (m, 2H, exocyclic -C=CH₂), 3.93 (s, 2H, benzylic CH₂); ¹³C NMR (75 MHz, Acetone-*d*₆) δ 169.06 (-CO), 164.25 (-CO), 162.03, 159.54, 156.55, 139.32, 134.07, 132.92, 132.28, 130.13, 125.71, 123.71, 120.58, 118.70, 117.01, 116.71, 95.24 (exocyclic -C=CH₂), 32.27 (benzylic CH₂); ESI-MS *m/z*: 372.3 [M+Na]⁺; ESI-HRMS *m/z*: 350.1198 [M+H]⁺, calcd for C₂₁H₁₇FNO₃ 350.1187.

5.1.3.14.

(*E*)-3-(3-Fluorophenyl)-*N*-(4-((2-methylene-5-oxo-2,5-dihydrofuran-3-yl)methyl)phenyl)acrylamide (**B-14**). White solid, mp 122.9-123.7 °C, yield 77%; ¹H NMR (300 MHz, Acetone-*d*₆) δ 9.49 (s, 1H, N-H), 7.77 (d, *J* = 8.4 Hz, 2H, Ar-H), 7.67 (d, *J* = 15.6 Hz, 1H, -C=CH), 7.50 – 7.44 (m, 2H, Ar-H), 7.39 (d, *J* = 10.5 Hz, 1H, Ar-H), 7.30 (d, *J* = 8.4 Hz, 2H, Ar-H), 7.20 – 7.13 (m, 1H, Ar-H), 6.89 (d, *J* = 15.6 Hz, 1H, -C=CH), 6.02 (s, 1H, -C=CH), 5.20 – 5.14 (m, 2H, exocyclic -C=CH₂), 3.93 (s, 2H, benzylic CH₂); ¹³C NMR (75 MHz, Acetone-*d*₆) δ 169.05 (-CO), 165.66 (-CO), 164.08, 159.54, 156.55, 140.26, 139.29, 138.56, 132.94, 131.65, 130.14, 124.84, 124.44, 120.56, 118.70, 117.13, 114.70, 95.24 (exocyclic -C=CH₂), 32.27 (benzylic CH₂); ESI-MS *m/z*: 348.3 [M-H]⁻; ESI-HRMS *m/z*: 350.1199 [M+H]⁺, calcd for C₂₁H₁₇FNO₃ 350.1187.

5.1.3.15.

(*E*)-3-(4-Fluorophenyl)-*N*-(4-((2-methylene-5-oxo-2,5-dihydrofuran-3-yl)methyl)phenyl)acrylamide (**B-15**). White solid, mp 100.9-101.9 °C, yield 71%; ¹H NMR (300 MHz, Acetone-*d*₆) δ 9.50 (s, 1H, N-H), 7.77 (d, *J* = 8.4 Hz, 2H, Ar-H), 7.70 – 7.63 (m, 3H, -C=CH, Ar-H), 7.29 (d, *J* = 8.4 Hz, 2H, Ar-H), 7.18 (t, *J* = 8.7 Hz, 2H, Ar-H), 6.81 (d, *J* = 15.6 Hz, 1H, -C=CH), 6.01 (s, 1H, -C=CH), 5.17 (s, 2H, exocyclic -C=CH₂), 3.92 (s, 2H, benzylic CH₂); ¹³C NMR (75 MHz, Acetone-*d*₆) δ 169.02 (-CO), 165.95 (-CO), 164.38, 159.56, 156.54, 140.38, 139.29, 132.80, 132.52, 130.74, 130.11, 122.80, 120.54, 118.68, 116.65, 95.25 (exocyclic -C=CH₂), 32.15 (benzylic CH₂); ESI-MS *m/z*: 372.3 [M+Na]⁺; ESI-HRMS *m/z*: 350.1185 [M+H]⁺, calcd for C₂₁H₁₇FNO₃ 350.1187.

5.2.1. DNA Topo I Mediated Relaxation Assay *in vitro*

DNA Topo I inhibitory assay was conducted using a previously reported method [7]. The tested compounds were previously dissolved in DMSO at a concentration of 100 mM as stock solutions. CPT was used as a positive control. A mixture of 0.1 μg pBR322 DNA (TaKaRa, Kyoto, Japan) and 0.2 units of recombinant human Topo I was incubated in the presence or absence of the prepared compounds at 37 °C for 30 min in the Topo I buffer (20 mL) which was provided by the supplier (TaKaRa, Kyoto, Japan). The reaction was terminated by the addition of a dye solution containing 0.25% bromophenol blue, 0.25% xylene cyanol ff and 40% glycerol. Then samples were electrophoresed on a 1% agarose gel at 100 V for 30 min in a running buffer of 1 x TAE buffer (40 mM Tris-acetate, 2 mM EDTA, 19.9 mM HOAc). Gels were stained for 30 min in 200 mL 1 x TAE buffer containing ethidium bromide (0.5 μg/mL) and destained with 200 mL double distilled water for 20 min. DNA bands were visualized by transillumination with UV light and quantitated using an Alpha Imager (Alpha Innotech Corporation).

5.2.2. Anticancer activity *in vitro* by MTT

To measure the antiproliferative activity of the compounds in various cancer cell lines, cell viability was assessed by a classical MTT assay [30]. Three human cancer cell lines, MCF-7 (human breast adenocarcinoma cell line), HeLa (human cervix tumor cell line), A549 (adenocarcinomic human alveolar basal epithelial cell line)

were used in this study. The cells were seeded in 96-well plates at a density of 3.5×10^3 per well and incubated overnight in 100 μL of a medium containing 10% Fetal Bovine Serum (Gibco, USA). On the following day, the culture medium in each well was replaced by fresh medium containing a range of concentrations of the 4-(4-substituted amidobenzyl)furan-2(5H)-one derivatives for a cultivation lasting 48 h. Then 20 μL of 5 mg/mL MTT solution were added into each well with a subsequent incubation for 4 h at 37 $^{\circ}\text{C}$. Culture medium was then removed, and 200 μL DMSO was added to dissolve the formazan dye. The absorption was determined by a microplate-reader (Bio-Tek) at 570 nm. Parallel triplicate repetition for each dose was made.

5.2.3. DNA-insertion assay

The DNA-insertion assay was performed in 20 μL of Topo I buffer (50 mM Tris-HCl, pH 7.5, 10 mM MgCl_2 , 50 mM KCl, 0.1 mM EDTA, 0.5 mM DTT, and 30 mg/mL bovine serum albumin) containing 0.1 μg supercoiled pBR322DNA and excess Topo I (4 units). The DNA was pre-incubated with different compounds at 25 $^{\circ}\text{C}$ for 10 min. Then Topo I was added to initiate the reaction for 30 min at 37 $^{\circ}\text{C}$. Afterwards 4 μL of 6 x DNA loading buffer (0.25% bromophenol blue, xylene cyanol ff 0.25% and 40% glycerol) were added into the samples and electrophoresed for 40 min in a 1% agarose gel in 1 x TAE buffer (40 mM Tris-acetate, 2 mM EDTA, 19.9 mM HOAc). Finally the gels were stained for 30 min in 200 mL 1 x TAE buffer containing EB (0.5 μg /mL), and destained for 20 min with 200 mL double distilled water. DNA bands were visualized by transillumination with UV light and photographed by an Alpha Innotech digital imaging system.

5.2.4. Topo I-mediated DNA cleavage assay

DNA cleavage assay was carried as follows. 0.125 μg supercoiled pBR322DNA was incubated with 7.5 units Topo I in 10 μL of Topo I buffer (50 mM Tris-HCl, pH 7.5, 50 mM KCl, 10 mM MgCl_2 , 0.5 mM DTT, 0.1 mM EDTA, and 30 mg/mL bovine serum albumin) at 37 $^{\circ}\text{C}$ for 30 min in the presence of tested compounds. After 30 min, the reaction was stopped by adding 1% SDS and 0.8 mg/mL proteinase K. An additional incubation for 10 min at 50 $^{\circ}\text{C}$ to digest the Topo I was necessary before

samples were mixed with 2 μL of 6 x loading buffer (0.25% bromophenol blue, xylene cyanol ff 0.25% and 40% glycerol), and electrophoresed in 1% agarose gel in 1 x TAE buffer (40 mM tris-acetate, 2 mM EDTA, 19.9 mM HOAc) for 60 min at 60 V after. Then gels were stained by 200 mL 1 x TAE containing 0.5 $\mu\text{g}/\text{mL}$ EB for 30 min and a secondary electrophoresis of 30 min was significant to separate the relaxed DNA and nicked DNA. DNA bands were visualized by transillumination with UV light, photographed by an Alpha Innotech digital imaging system.

5.2.5. EMSA assay

The DNA mobility shift assay was performed as described in a paper with minor modifications [26]. First Topo I (4 units) was added into 10 μL of Topo I buffer (50 mM Tris-HCl, pH 7.5, 50 mM KCl, 10 mM MgCl_2 , 0.5 mM DTT, 0.1 mM EDTA, and 30 mg/mL bovine serum albumin), which was incubated in the absence or in the presence of compounds at 25 $^\circ\text{C}$ for 20 min. Then 0.1 μg of pBR322 DNA was added as another incubation for 3 min. The samples were immediately analyzed using a 1% agarose gel with 1% EB at 1 V/cm for 8 h on ice. Finally, DNA bands were visualized by transillumination with UV light, photographed by an Alpha Innotech digital imaging system.

5.3. Molecular docking

Sybyl-8.1 surflex-dock module (Tripos, Inc. St. Louis, MO) was used in molecular docking, and the structure of Topo I was downloaded from the Protein Data Bank (PDB: 1K4T). The water and small molecule ligands were removed with other necessary modification in order to create a simulated physiological environment. A threshold parameter of 0.5 and a bloat parameter of 0 \AA were set to generate the protomol, which is a computational representation of a ligand that makes every potential interaction with the binding site, and the Kollman all-charges were added. We then conducted the staged minimization with 100 steps at every stage and applied GeomX model mode to the docking study. Sequentially all of our compounds were docked into the binding site. Minimum RMSD between final poses and other parameters were respectively set as 0.5 \AA to distinguish conformations and default.

After docking study, the binding conformation with highest score was subjected to MD simulations in AMBER molecular dynamics package [31]. The total MD time was 20 ns in explicit solvent. We used the Antechamber tool to generate the partial atomic charges of each ligand and the AMBER force field ff12SB [32] were loaded. The complexes were then immersed in a truncated octahedral water box by the TIP3P water model before minimization and MD. Analysis was performed with the ptraj analysis tool based on the last 2ns trajectories of the simulation. The binding free energies of complexes were calculated using the MM-PBSA.

Acknowledges

We sincerely thank the Natural Science Foundation of China (81273362) for financial support of this study.

Reference

- [1] P. Vineis, C.P. Wild, Global cancer patterns: causes and prevention, *Lancet*. 383 (2014) 549-557.
- [2] R. Siegel, D. Naishadham, A. Jemal, Cancer statistics, 2013, *CA: Cancer J. Clin.* 63 (2013) 11-30.
- [3] M. Gupta, A. Fujimori, Y. Pommier, Eukaryotic DNA topoisomerases I, *Biochim. Biophys. Acta*. 1262 (1995) 1-14.
- [4] J.C. Wang, DNA topoisomerases, *Annu. Rev. Biochem.* 65 (1996) 635-692.
- [5] T.D. Pfister, W.C. Reinhold, K. Agama, S. Gupta, S.A. Khin, R.J. Kinders, R.E. Parchment, J.E. Tomaszewski, J.H. Doroshow, Y. Pommier, Topoisomerase I levels in the NCI-60 cancer cell line panel determined by validated ELISA and microarray analysis and correlation with indenoisoquinoline sensitivity, *Mol. Cancer Ther.* 8 (2009) 1878-1884.
- [6] M.S. Braun, S.D. Richman, P. Quirke, C. Daly, J.W. Adlard, F. Elliott, J.H. Barrett, P. Selby, A.M. Meade, R.J. Stephens, M.K.B. Parmar, M.T. Seymour, Predictive biomarkers of chemotherapy efficacy in colorectal cancer: Results from the UK MRC FOCUS trial, *J. Clin. Oncol.* 26 (2008) 2690-2698.
- [7] W. Hou, Z.-Y. Wang, C.-K. Peng, J. Lin, X. Liu, Y.-Q. Chang, J. Xu, R.-W. Jiang, H. Lin, P.-H. Sun, W.-M. Chen, Novel securinine derivatives as topoisomerase I based antitumor agents, *Eur. J. Med. Chem.* 122 (2016) 149-163.
- [8] I. Husain, J.L. Mohler, H.F. Seigler, J.M. Besterman, Elevation of topoisomerase I messenger RNA, protein, and catalytic activity in human tumors: Demonstration of tumor-type specificity and implications for cancer chemotherapy, *Cancer Res.* 54 (1994) 539-546.
- [9] J.M. Calderón-Montano, E. Burgos-Morón, M.L. Orta, N. Pastor, C.A. Austin, S. Mateos, M. López-Lázaro, Alpha, beta-unsaturated lactones 2-furanone and 2-pyrone induce cellular DNA damage, formation of topoisomerase I- and II-DNA complexes and cancer cell death, *Toxicol. Lett.* 222 (2013) 64-71.

- [10] K. Bielawski, K. Winnicka, A. Bielawska, Inhibition of DNA Topoisomerases I and II, and growth inhibition of breast cancer MCF-7 cells by ouabain, digoxin and proscillaridin A, *Biol. Pharm. Bull.* 29 (2006) 1493-1497.
- [11] S. Takahashi, Y. Yonezawa, A. Kubota, N. Ogawa, K. Maeda, H. Koshino, T. Nakata, H. Yoshida, Y. Mizushima, Pyranicin, a non-classical annonaceous acetogenin, is a potent inhibitor of DNA polymerase, topoisomerase and human cancer cell growth, *Int. J. Oncol.* 2008, pp. 451-458.
- [12] Q. Zhang, Y. Lu, Y. Ding, J. Zhai, Q. Ji, W. Ma, M. Yang, H. Fan, J. Long, Z. Tong, Y. Shi, Y. Jia, B. Han, W. Zhang, C. Qiu, X. Ma, Q. Li, Q. Shi, H. Zhang, D. Li, J. Zhang, J. Lin, L.Y. Li, Y. Gao, Y. Chen, Guaianolide sesquiterpene lactones, a source to discover agents that selectively inhibit acute myelogenous leukemia stem and progenitor cells, *J. Med. Chem.* 55 (2012) 8757-8769.
- [13] S. Neelakantan, S. Nasim, M.L. Guzman, C.T. Jordan, P.A. Crooks, Aminoparthenolides as novel anti-leukemic agents: Discovery of the NF- κ B inhibitor, DMAPT (LC-1), *Bioorg. Med. Chem. Lett.* 19 (2009) 4346-4349.
- [14] D.S. Kim, C.G. Dong, J.T. Kim, H. Guo, J. Huang, P.S. Tiseni, Y. Kishi, New syntheses of E7389 C14-C35 and halichondrin C14-C38 building blocks: double-inversion approach, *J. Am. Chem. Soc.* 131 (2009) 15636-15641.
- [15] A.D. Ricart, Antibody-drug conjugates of calicheamicin derivative: gemtuzumab ozogamicin and inotuzumab ozogamicin, *Clin. Cancer Res.* 17 (2011) 6417-6427.
- [16] V.I. Murav'eva, A.I. Ban'kovskii, Chemical study of alkaloids of *Securinega suffruticosa*, *Doklady Akademii Nauk SSSR.* 110 (1956) 998-1000.
- [17] Y.H. Xia, C.R. Cheng, S.Y. Yao, Q. Zhang, Y. Wang, Z.N. Ji, L-Securinine induced the human colon cancer SW480 cell autophagy and its molecular mechanism, *Fitoterapia.* 82 (2011) 1258-1264.
- [18] S. Rana, K. Gupta, J. Gomez, S. Matsuyama, A. Chakrabarti, M.L. Agarwal, A. Agarwal, M.K. Agarwal and D.N. Wald, Securinine induces p73-dependent apoptosis preferentially in p53-deficient colon cancer cells, *The FASEB Journal • Res. Com.* 24 (2010) 2126-2134.

- [19] S. Laugraud, A. Guingant, J. d'Angelo, A Direct Route for the Synthesis of (*E*)-3-Alkyl-4-oxo-2-butenamide Esters, *J. Org. Chem.* 52 (1987) 4788-4790.
- [20] G. Hughes, M. Kimura, S.L. Buchwald, Catalytic enantioselective conjugate reduction of lactones and lactams, *J. Am. Chem. Soc.* 125 (2003) 11253-11258.
- [21] G. Liu, B.G. Szczepankiewicz, Z. Pei, Z. Xin, T.K. Oost, D.A. Janowick, Preparation of amino(oxo)acetic acids as protein tyrosine phosphatase inhibitors, WO2002018323A2, 2002.
- [22] R. Buyle, H.G. Viehe, α -Chloroamines. IV. Aminated heterocycles from the reaction of phosgene with substituted acetamides, *Tet. Lett.* 25 (1969) 3453-3459.
- [23] G. Iskander, R. Zhang, D.S.-H. Chan, D.S. Black, M. Alamgir, N. Kumar, An efficient synthesis of brominated 4-alkyl-2(5H)-furanones, *Tet. Lett.* 50 (2009) 4613-4615.
- [24] J.C. Wang, The degree of unwinding of the DNA helix by ethidium. I. Titration of twisted PM2 DNA molecules in alkaline cesium chloride density gradients, *J. Mol. Biol.* 89 (1974) 783-801.
- [25] B.L. Staker, K. Hjerrild, M.D. Feese, C.A. Behnke, A.B. Burgin, Jr., L. Stewart, The mechanism of topoisomerase I poisoning by a camptothecin analog, *Proc. Natl. Acad. Sci. U. S.A.* 99 (2002) 15387-15392.
- [26] J.J. Champoux, DNA topoisomerases: structure, function, and mechanism, *Annu. Rev. Biochem.* 70 (2001) 369-413.
- [27] Y. Pommier, J.M. Covey, D. Kerrigan, J. Markovits, R. Pham, DNA unwinding and inhibition of mouse leukemia L1210 DNA topoisomerase I by intercalators, *Nucleic. Acids. Res.* 15 (1987) 6713-6731.
- [28] G.L. Beretta, P. Perego, F. Zunino, Targeting topoisomerase I: molecular mechanisms and cellular determinants of response to topoisomerase I inhibitors, *Expert Opin. Ther. Targets.* 12 (2008) 1243-1256.
- [29] F. Boege, T. Straub, A. Kehr, C. Boesenberg, K. Christiansen, A. Andersen, F. Jakob, J. Kohrle, Selected novel flavones inhibit the DNA binding or the DNA religation step of eukaryotic topoisomerase I, *J. Biol. Chem.* 271 (1996) 2262-2270.

- [30] M.S. Zheng, Y.K. Lee, Y. Li, K. Hwangbo, C.S. Lee, J.R. Kim, S.K. Lee, H.W. Chang, J.K. Son, Inhibition of DNA topoisomerases I and II and cytotoxicity of compounds from *Ulmus davidiana* var. *japonica*, *Arch. Pharm. Res.* 33 (2010) 1307-1315.
- [31] D.A. Case, T. Darden, T.E. Cheatham III, C.L. Simmerling, J. Wang, R.E. Duke, R. Luo, R.C. Walker, W. Zhang, K.M. Merz, B.P. Roberts, S. Hayik, A. Roitberg, G. Seabra, J. Swails, A.W. Goetz, I. Kolossvai, K.F. Wong, F. Paesani, J. Vanicek, R.M. Wolf, J. Liu, X. Wu, S.R. Brozell, T. Steinbrecher, H. Gohlke, Q. Cai, X. Ye, B. Wang, M.J. Hsieh, G. Cui, D.R. Roe, D.H. Mathews, M.G. Seetin, R. Salomon-Ferrer, C. Sagui, V. Babin, T. Luchko, S. Gusarov, A. Kovalenko, P.A. Kollman. AMBER 12. University of California, San Francisco (2012).
- [32] T.E. Cheatham, 3rd, P. Cieplak, P.A. Kollman, A modified version of the force field with improved sugar pucker phases and helical repeat, *J. Biomol. Struct. Dyn.* 16 (1999) 845-862.

Figure Captions

Figure 1. Design strategy of 4-(4-substituted amido-benzyl)furan-2(5H)-one derivatives.

Figure 2. (A) Topo I inhibitory activity of 4-(4-substituted amidobenzyl) furan-2(5H)-one derivatives. CPT is a positive control. Supercoiled pBR322 DNA was incubated with Topo I in the presence or absence of 4-(4-substituted amidobenzyl)furan-2(5H)-one derivatives at 37 °C for 30 min. Lane A is pBR322 DNA only. Lane B is the mixture of pBR322 DNA and Topo I. Lane C is the mixture of pBR322 DNA, Topo I and 100 μM CPT. Other lanes are the mixture of pBR322 DNA, Topo I and 100 μM 4-(4-substituted amidobenzyl)furan-2(5H)-one derivatives; (B) The gray scale value analysis of A.

Figure 3. (A) Topo I inhibitory activity of different concentration of **B-15**. Supercoiled pBR322 DNA was incubated with Topo I in the presence or absence of **B-15** at 37 °C for 30 min. Lane A is pBR322 DNA only. Lane B is the mixture of pBR322 DNA and Topo I. Other lanes are the mixture of pBR322 DNA, Topo I and 200, 150, 100, 75, 50, 25, 12.5, 6.25, 3.125, 1 μM **B-15**; (B) The gray scale value analysis of A.

Figure 4. The π - π stacking interactions and π -alkyl stacking interaction between Topo I and the furanone ring of compounds **B-13** (A), **B-14** (B), **B-15** (C). The π - π stacking interaction and π -alkyl stacking interaction are shown as red and blue dashed lines respectively.

Figure 5. The relaxation process of Topo I for supercoiled DNA and mechanism of Topo I inhibitors, including CPT and **B-15**.

Figure 6. DNA-insertion assay of pure compounds of series **2**. Ethidium bromide (EB) is a positive control. Supercoiled pBR322 DNA was incubated with Topo I in the presence or absence of EB, CPT, and the tested compounds at 37 °C for 30 min. Lane A is pBR322 DNA only. Lane B is the mixture of pBR322 DNA and Topo I. Lane C is the mixture of pBR322 DNA, Topo I and 100 μM CPT. Lane E is the mixture of pBR322 DNA, Topo I and 25 μM EB. Other lanes are the mixture of pBR322 DNA, Topo I and 100 μM tested compounds.

Figure 7. (A) Topo I-mediated DNA cleavage assay of pure compounds **B-15**. CPT is a positive control. Lane A is pBR322 DNA only. Lane B is the mixture of pBR322 DNA and Topo I. Other lanes are the mixture of pBR322 DNA, Topo I and 25, 50 μM CPT or 25, 50, 100, 200, 400 μM **B-15**; (B) The gray scale value analysis of A.

Figure 8. (A) EMSA-assay of pure compounds **B-15**. CPT is a negative control. Lane A is pBR322 DNA only. Lane B is the mixture of pBR322 DNA and Topo I. Lane C is the mixture of pBR322 DNA, Topo I and 50 or 100 μM CPT. Other lanes are the mixture of pBR322 DNA, Topo I and 50, 100, 200, 300, 400 μM **B-15**; (B) The gray scale value analysis of A.

Figure 9. (A) Hypothetical binding modes between Topo I (1K4T) and **B-15** (the H-bonds are illustrated as green dashed lines); (B) The π - π stacking interaction and the π -alkyl stacking interaction between Topo I and **B-15** (the π - π stacking interaction and the π -alkyl stacking interaction are illustrated as red and blue dashed lines respectively). (C) Hypothetical binding modes between Topo I (1K4T) from PDB (DNA was removed) and **B-15**. (The H-bonds are illustrated as green dashed lines).

Figure 10. (A) Binding model between **B-13** and Topo I from docking and molecular dynamics; (B) Binding model between **B-14** and Topo I from docking and molecular dynamics; (C) Binding model between **B-15** and Topo I from docking and molecular dynamics.

Table 1. Gray scale value analysis of **Figure 2**

Compounds	Topo I inhibition rate(%) ^a vs control	Compounds	Topo I inhibition rate(%) ^a vs control
CPT ^b	79.50±0.23	B-5	41.93±0.88
A-1	19.43±0.74	B-6	34.93±1.02
A-2	20.33±0.26	B-7	32.82±0.99
A-3	12.35±1.10	B-8	43.32±0.63
A-4	11.00±0.71	B-9	21.27±0.82
A-5	11.65±0.63	B-10	22.53±0.39
A-6	13.07±0.76	B-11	30.28±0.83
A-7	12.05±0.16	B-12	48.64±0.29
B-1	28.69±0.81	B-13	44.62±0.80
B-2	28.49±0.69	B-14	34.53±0.93
B-3	47.94±0.89	B-15	94.05±0.64
B-4	32.31±0.18		

^a All data represent mean ± S.D. from different experiments performed in triplicate.

^b CPT acted as a positive control.

Table 2. Cytotoxicity of 4-(4-substituted amidobenzyl)furan-2(5H)-one derivatives against cancer cell lines

Compounds	IC ₅₀ (μM) ^a		
	MCF-7	Hela	A549
CPT^b	71.30±0.21	60.01±1.01	0.24±0.19
A-1	49.19±0.95	>50	41.38±0.47
A-2	43.81±1.01	44.61±0.81	48.92±2.00
A-3	40.11±2.02	43.99±0.69	>50
A-4	46.39±0.77	48.83±1.73	45.82±2.51
A-5	>50	45.82±2.28	40.00±2.66
A-6	39.01±2.84	49.01±1.20	>50
A-7	47.91±0.75	>50	41.81±2.39
B-1	>50	48.32±7.23	49.83±1.72
B-2	>50	>50	39.01±2.91
B-3	3.94±0.78	7.12±0.36	7.79±1.61
B-4	48.72±6.02	37.47±5.90	37.51±1.61
B-5	6.15±1.28	8.63±0.49	6.69±0.34
B-6	39.82±6.82	39.67±4.39	42.93±0.84
B-7	48.29±3.81	40.49±1.47	31.97±0.99
B-8	15.98±0.63	16.17±0.34	22.8±1.39
B-9	40.91±1.92	42.57±2.43	48.77±0.86
B-10	42.92±5.02	45.82±1.49	40.99±2.18
B-11	37.42±0.38	35.54±1.93	37.64±0.79
B-12	9.49±0.40	7.34±0.63	14.77±0.92
B-13	13.77±1.19	6.93±1.40	7.41±1.25
B-14	39.01±1.91	30.24±0.87	35.24±1.28
B-15	4.43±0.14	2.77±1.12	3.46±1.29

^a All data represent mean ± S.D. from different experiments performed in triplicate.

^b CPT acted as a positive control for MTT assay.

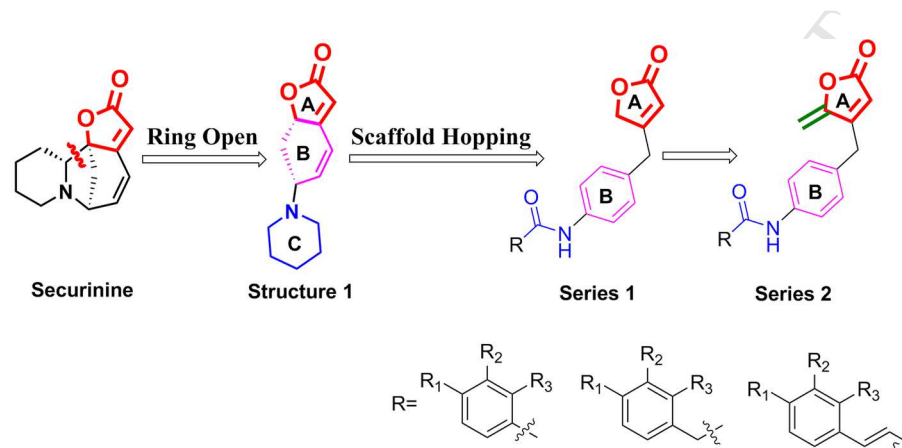


Figure 1. Design strategy of 4-(4-substituted amido-benzyl)furan-2(5H)-one derivatives

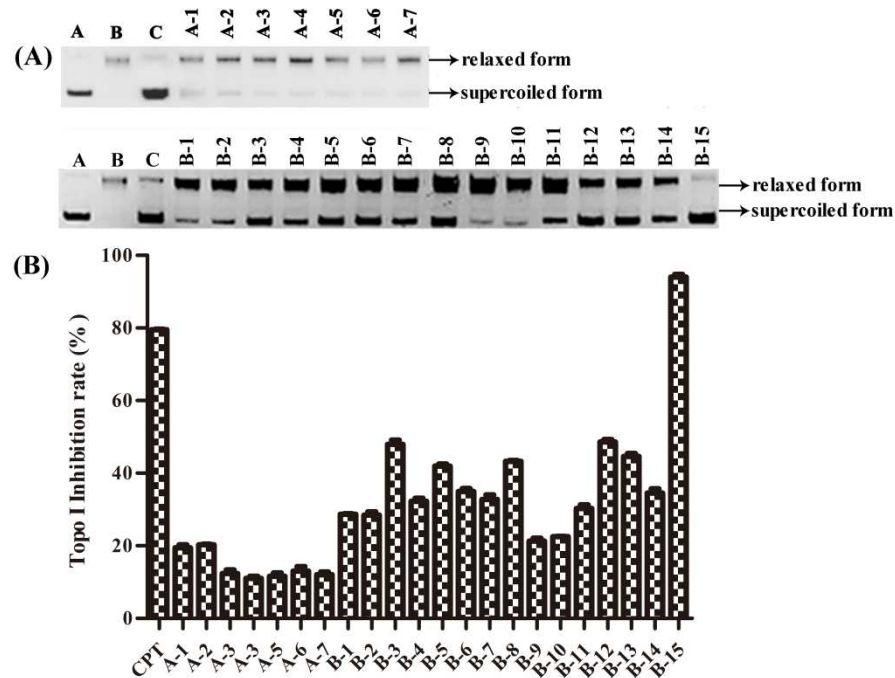


Figure 2. (A) Topo I inhibitory activity of 4-(4-substituted amido-benzyl)furan-2(5H)-one derivatives. CPT is a positive control. Supercoiled pBR322 DNA was incubated with Topo I in the presence or absence of 4-(4-substituted amidobenzyl)furan-2(5H)-one derivatives at 37 °C for 30 min. Lane A is pBR322 DNA only. Lane B is the mixture of pBR322 DNA and Topo I. Lane C is the mixture of pBR322 DNA, Topo I and 100

μM CPT. Other lanes are the mixture of pBR322 DNA, Topo I and 100 μM 4-(4-substituted amido-benzyl)furan-2(5H)-one derivatives; **(B)** The gray scale value analysis of A.

ACCEPTED MANUSCRIPT

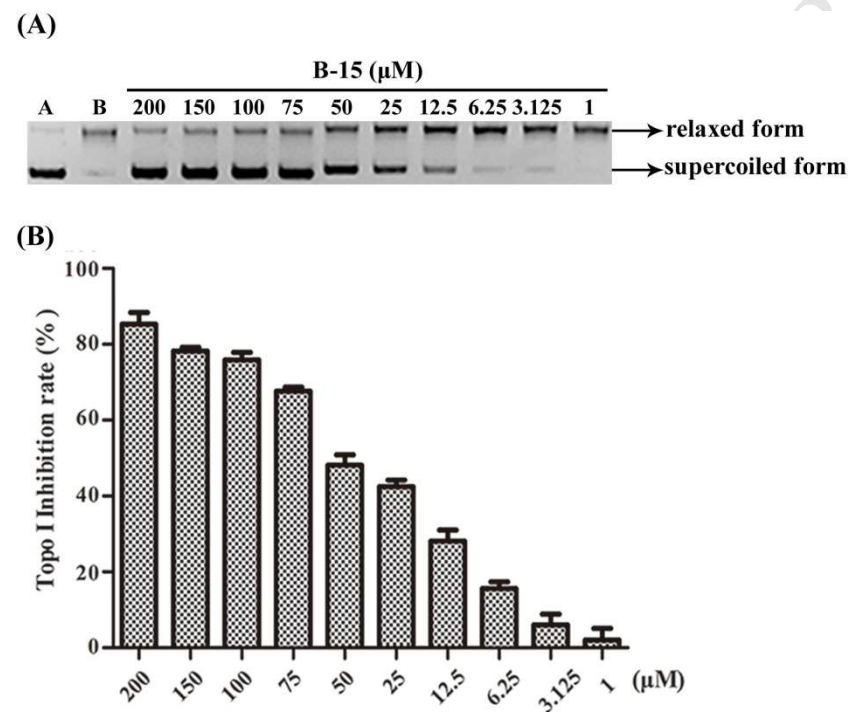


Figure 3. (A) Topo I inhibitory activity of different concentration of **B-15**. Supercoiled pBR322 DNA was incubated with Topo I in the presence or absence of **B-15** at 37 °C for 30 min. Lane A is pBR322 DNA only. Lane B is the mixture of pBR322 DNA and Topo I. Other lanes are the mixture of pBR322 DNA, Topo I and 200, 150, 100, 75, 50, 25, 12.5, 6.25, 3.125, 1 μM **B-15**. (B) The gray scale value analysis of A.

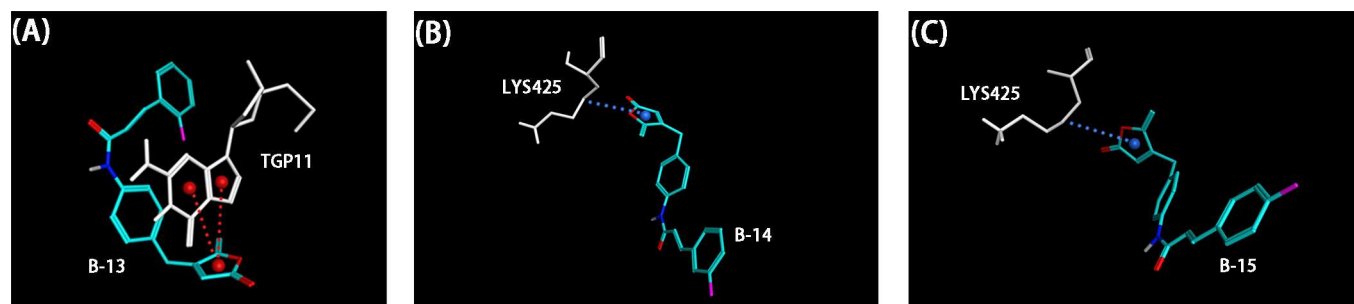


Figure 4. The π - π stacking interactions and π -alkyl stacking interaction between Topo I and the furanone ring of compounds **B-13** (A), **B-14** (B), **B-15** (C). The π - π stacking interaction and π -alkyl stacking interaction are shown as red and blue dashed lines respectively.

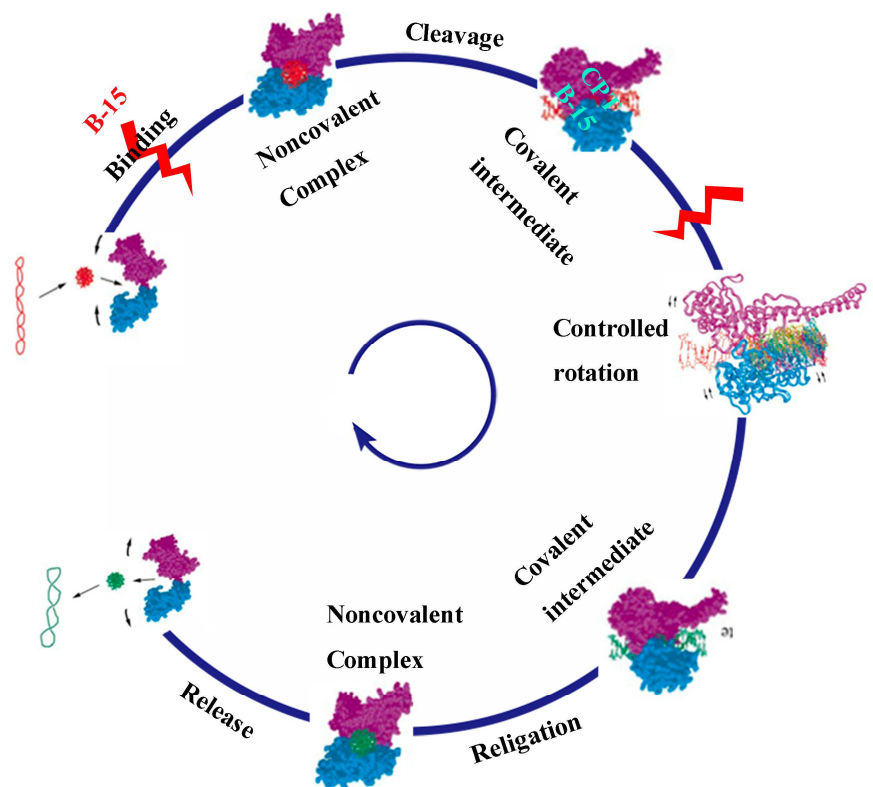


Figure 5. The relaxation process of Topo I for supercoiled DNA and mechanism of Topo I inhibitors including CPT and **B-15**.

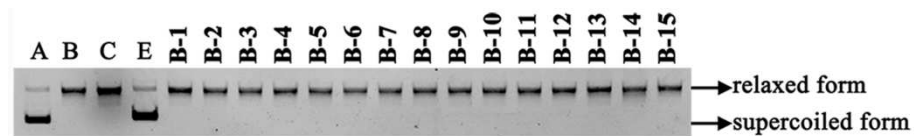


Figure 6. DNA-insertion assay of pure compounds of series **2**. Ethidium bromide (EB) is a positive control. Supercoiled pBR322 DNA was incubated with Topo I in the presence or absence of EB, CPT, and the tested compounds at 37 °C for 30 min. Lane A is pBR322 DNA only. Lane B is the mixture of pBR322 DNA and Topo I. Lane C is the mixture of pBR322 DNA, Topo I and 100 μ M CPT. Lane E is the mixture of pBR322 DNA, Topo I and 25 μ M EB. Other lanes are the mixture of pBR322 DNA, Topo I and 100 μ M tested compounds.

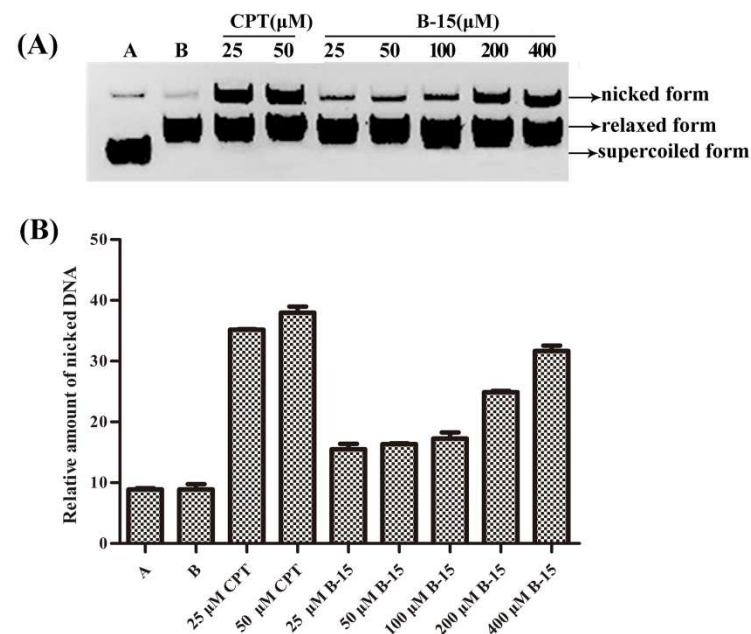


Figure 7. (A) Topo I-mediated DNA cleavage assay of pure compounds **B-15**. CPT is a positive control. Lane A is pBR322 DNA only. Lane B is the mixture of pBR322 DNA and Topo I. Other lanes are the mixture of pBR322 DNA, Topo I and 25, 50 μ M CPT or 25, 50, 100, 200, 400 μ M **B-15**; (B) The gray scale value analysis of A.

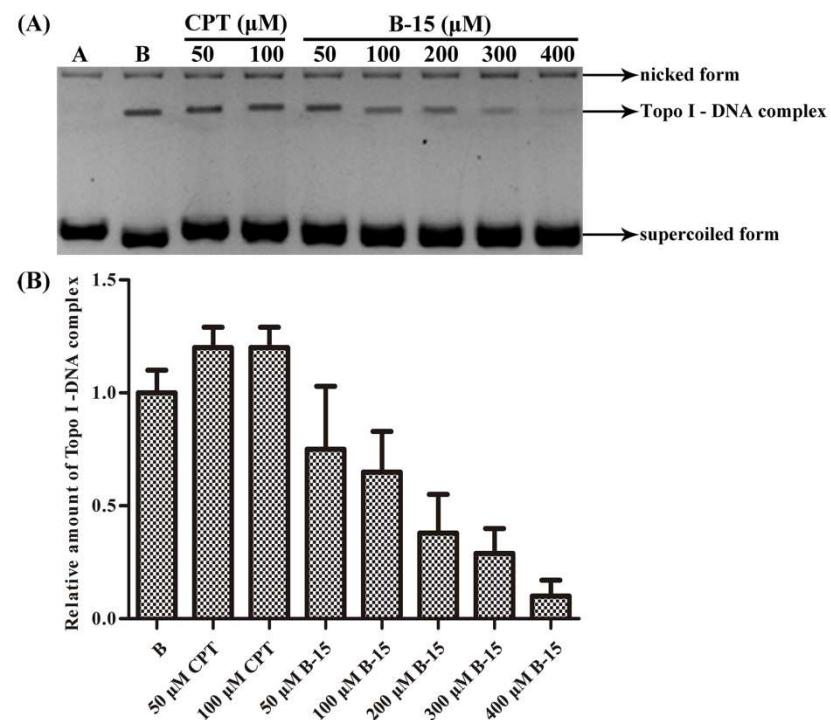


Figure 8. (A) EMSA-assay of pure compounds **B-15**. CPT is a negative control. Lane A is pBR322 DNA only. Lane B is the mixture of pBR322 DNA and Topo I. Line C is the mixture of pBR322 DNA, Topo I and 50 or 100 μM CPT. Other lanes are the mixture of pBR322 DNA, Topo I and 50, 100, 200, 300, 400 μM **B-15**; (B) The gray scale value analysis of A.

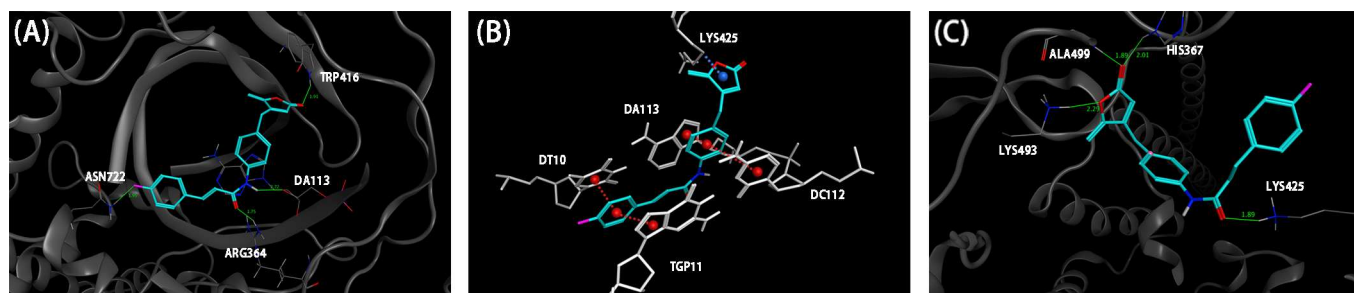


Figure 9. (A) Hypothetical binding modes between Topo I (1K4T) and **B-15** (the H-bonds are illustrated as green dashed lines); (B) The π - π stacking interaction and the π -alkyl stacking interaction between Topo I and **B-15** (the π - π stacking interaction and the π -alkyl stacking interaction are illustrated as red and blue dashed lines respectively). (C) Hypothetical binding modes between Topo I (1K4T) from PDB (DNA was removed) and **B-15**. (The H-bonds are illustrated as green dashed lines).

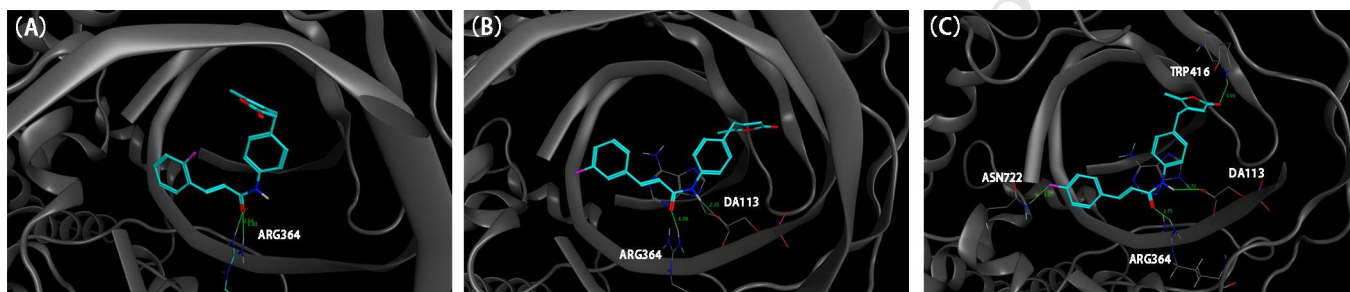
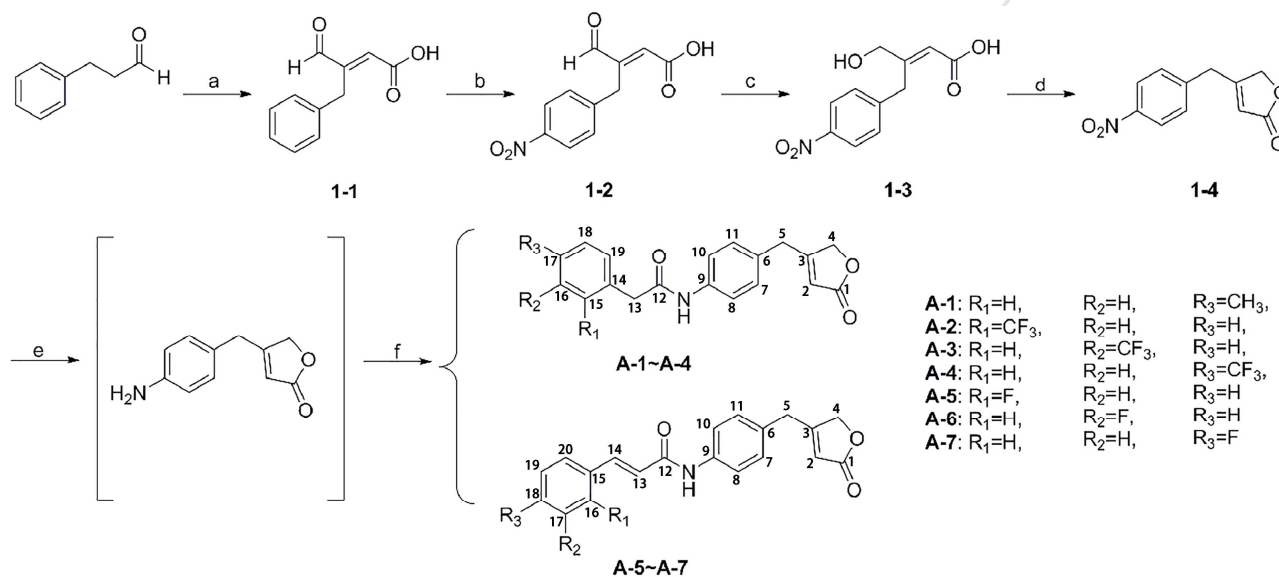
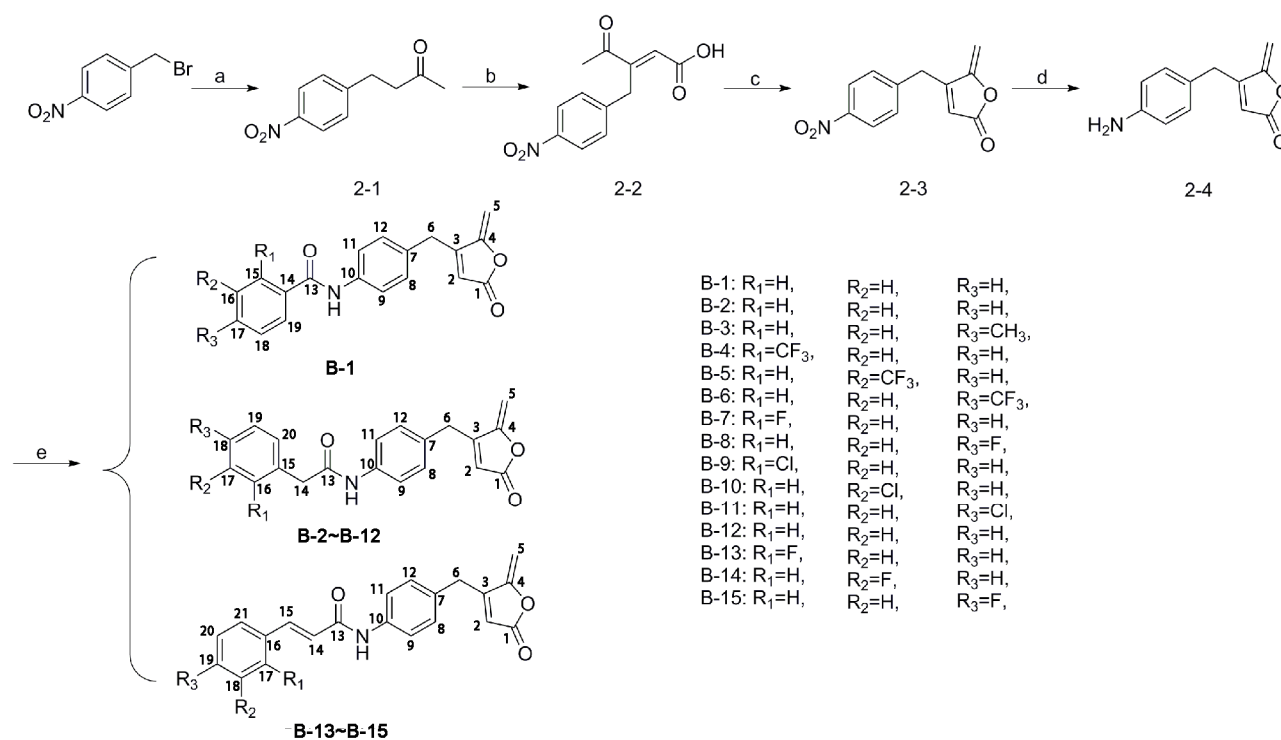


Figure10. (A) Binding model between **B-13** and Topo I from docking and molecular dynamics; (B) Binding model between **B-14** and Topo I from docking and molecular dynamics; (C) Binding model between **B-15** and Topo I from docking and molecular dynamics.



Scheme 1. Synthetic route to 4-(4-substituted amidobenzyl)furan-2(5H)-one derivatives **A-1~A-7**. Reagents and conditions: (a) glyoxylic acid monohydrate, KOH, MeOH, room temperature, 4 h; (b) nitrosonitric acid, -10 °C, 4 h; (c) sodium borohydride, MeOH, 0 °C, 2 h (d) EDCI, CH₂Cl₂/Et₃N, room temperature, 2 h (e) Fe, NH₄Cl, THF /H₂O, reflux; (f) acyl chloride, pyridine, THF, 0 °C to room temperature, 30 min.



Scheme 2. Synthetic route to 4-(4-substituted amidobenzyl)furan-2(5H)-one derivatives **B-1~B-15**. Reagents and conditions: (a) 2,4-pentanedione, K₂CO₃, MeOH, reflux, 4h; (b) glyoxylic acid monohydrate, phosphoric acid, 85 °C, 4 h; (c) p-TsOH, toluene, reflux; (d) Fe, NH₄Cl, THF/H₂O, reflux; (e) acyl chloride, pyridine, THF, 0 °C to room temperature, 30 min.

Highlights

1. Two series of 4-(4-substituted amido-benzyl)furan-2(5H)-one derivatives were synthesized based on the structural simplification of securinine.
2. Compounds bearing an exocyclic double bond on the furanone ring showed significant Topo I inhibitory and potent anti-proliferative activity.
3. Dual action mechanisms were identified for this class of compounds.